E. Aas

1

KØBENHAVNS UNIVERSITET

INSTITUT FOR FYSISK OCEANOGRAFI

ON SUBMARINE IRRADIANCE MEASUREMENTS

By

EYVIND AAS

OSLO

REPORT No. 6

COPENHAGEN 1969

KØBENHAVNS UNIVERSITET

INSTITUT FOR FYSISK OCEANOGRAFI

ON SUBMARINE IRRADIANCE MEASUREMENTS

By

Eyvind Aas
Oslo

REPORT No. 6 COPENHAGEN 1969

ON SUBMARINE IRRADIANCE MEASUREMENTS

By

Eyvind Aas
Oslo

Abstract

The effects of the presence of oblique rays in filters and of immersion on the spectral sensitivity of an irradiance meter are investigated. The oblique rays may produce a distortion of the filter transmission curves, and the immersion causes a wavelength-dependent change in sensitivity. Irradiance data from four stations between Stadt and Trænabanken on the west coast of Norway are presented. The water masses are found to have vertical attenuations between coastal water 1 and ocean water II according to Jerlov's classification.

The instrument

An irradiance meter, similar to those described earlier by Petterson and Poole (1937) and Jerlov (1951, p. 9), is shown in detail on fig. 1. The letters on fig. 1 correspond to the following:

a) selenium cell (Evans Electroselenium Ltd.),
b) brass protecting case,
c) glass window,
d) lid,
e) rubber gasket
f) cable for the photo-current
g) colour filters,
h) opal glass
i) brass ring,
j) clamps

When the instrument is submerged the opal glass, the filters and one side of the window are wet. The instrument is mounted in a three-point support, and the electrical cable is connected with an external resistance of 10,100 or 1000 ohms, through which the circuit is closed. The voltage over the resistance is read off on a Knick Transistor Millivoltmeter mV31 with scales 0.15-150 mV, and thereby the current is calculated. The properties of the opal glass as a cosine collector were checked in air, and calculations on the results

show that for downward irradiance in the sea, the deviations from cosine collection are inconsequential. For upward irradiance on the other hand, the instrument will register too small values.

With an external resistance of 10 ohms the photocurrent seems to be a linear function of the irradiance up to 300 μA. With a 100 ohm resistance the photocurrent is linear to at least 100 μA. 1000 ohms are only used for currents under 1 μA.

The effect of oblique rays

The filters used were absorption filters of glass from Schott & Genossen, Jena. They are circular with a diameter of 8.5 cm and thickness of 2 mm. The transmission was measured on a Beckman spectrograph for a ray of normal incidence. However, under the opal glass some of the light reaching the photo cell will have an oblique path which alters the transmission value. The transmission inside the surface of the glass, θ, is given by

$$\theta(\lambda,j) = e^{-cz\ \sec j} = (\theta(\lambda,0))^{\sec j}$$

where λ is the wavelength of the ray, j is the angle of the refracted ray in glass, c is the attenuation coefficient and z is the thickness of the filter.

We see that greater j gives less transmission, because $\theta(o) \leq 1$. At the same time, the reflection losses at the boundary surfaces increase with increasing angle of incidence. We shall now try to find what influence these combined effects will have on the results.

Although the photocell is placed fairly close to the window (see fig. 1), and the diameter of the latter is large compared to the first (8.5:3,5), the center of the photocell is not likely to receive light with amgles of incidence greater than 80^{o}. Nevertheless, to make calculations easier, we shall assume that it receives light to 90^{o}, since the contribution from the last part

is very small (less than 1% of the total).

The irradiance E, that passes through one filter and the window, then becomes, in air,

$$E = \int_{2\pi} L(i)\, d\Omega_i \cos i\, \theta^{\sec j}\, \tfrac{1}{2}(\tau_p(i)^4 + \tau_s(i)^4)$$

$$= \int_{i=0}^{\pi/2} \int_{\phi=0}^{2\pi} L(i) \sin i\, di\, d\phi \cos i\, \theta^{\sec j}\, \tfrac{1}{2}(\tau_p(i)^4 + \tau_s(i)^4), \qquad (1)$$

where ϕ is the azimuth angle, L is the radiance from the overlying opal glass, i is the angle of incidence, $\theta=\theta(\lambda,0)$ and τ_p and τ_s are the transmission coefficients air/glass of the two components of light; the one with the electric vector parallel with the plane of incidence, and the one with electric vector perpendicular to it. We assume that the light leaving the opal glass is unpolarized. The functions $\tau(i)$ then becomes, after the well-known Freshel laws:

$$\tau_s(i) = \frac{\sin 2i \sin 2j}{\sin^2(i+j)}$$

$$\tau_p(i) = \frac{\tau_s(i)}{\cos^2(i-j)}$$

The angle i is connected with j through Snell's law of refraction:

$$n_i \sin i = n_j \sin j,$$

where n_i and n_j are the refractive indexes in the two media . In air $n_i = 1$.

The contribution from multiple reflection here is so small that it may be disregarded.

We now assume the opal glass to behave like a perfect diffuser, i.e. the radiance emitted is isotropic over the integration hemisphere. Equation (1) then transforms to

$$E = \Pi L \int_0^{\frac{\pi}{2}} \Theta^{\sec j} \tfrac{1}{2}(\tau_p^4 + \tau_s'^4) \sin 2i \, di$$

The total downward irradiance from the opal glass is

$$\Pi L \int_0^{\frac{\pi}{2}} \sin 2i \, di = \Pi L,$$

so that the irradiance transmission in air for diffuse light becomes

$$T_{da} = \int_0^{\frac{\pi}{2}} \Theta^{\sec j} \tfrac{1}{2}(\tau_p^4 + \tau_s^4) \sin 2i \, di$$

If we have two filters between the opal glass and the window, then τ is to be raised to the 6th power to account for all reflecting surfaces.

In water the reflection occurs on glass/water interfaces except on the lowest surface of the window. If we once again assume the radiance from the opal glass to be constant and unpolarized, we get the diffuse transmission

$$T_{dw} = \int_0^{\beta} \Theta \sec j \; \tfrac{1}{2}(\tau_{wp}(\alpha)^3 \, \tau_p(i) + \tau_{ws}(\alpha)^3 \, \tau_s(i)) \sin 2\alpha \, d\alpha, \tag{2}$$

where

β is the upper limit of transmission given by $n_w \sin \beta = n_j \sin \gamma = 1$, n_w is the refractive index of water, γ is the critical angle of total reflection glass/air, τ_w is the transmission coefficient of the water/glass interfaces and α is the angle of incidence in water.

By means of Snell's law

$$n_w \sin \alpha = n_j \sin j = 1 : \sin i,$$

equation (2) may be transformed to

$$T_{dw} = \int_0^{\frac{\pi}{2}} \Theta \sec j \; \tfrac{1}{2}(\tau_{wp}(\alpha)^3 \, \tau_p(i) + \tau_{ws}(\alpha)^3 \, \tau_s(i)) \frac{\sin 2i \; di}{n_w^2}$$

If we have two filters the τ_w's should be raised to the 5th power.

The integrals have been calculated on a computer with $n_w = 1.34$ and $n_j = 1.53$. In the spectrograph we measured the transmission values for a ray of normal incidence, T_{na}. For one filter

$$T_{na} = \Theta \; \tfrac{1}{2}(\tau_p(0)^2 + \tau_s(0)^2).$$

If we want the maximum values of T_{na} and T_{da} for one filter to be equal, that is $T_{da} = T_{na} = 0.914$ (for $\Theta = 1$), then

$$T_{dw} = \int_0^{\beta} \Theta \sec j \; \tfrac{1}{2}(\tau_{wp}(\alpha)^3 \, \tau_p(i) + \tau_{ws}(\alpha)^3 \, \tau_s(i)) \sin 2\alpha \, d\alpha, \qquad (2)$$

where

β is the upper limit of transmission given by $n_w \sin \beta = n_j \sin \gamma = 1$, n_w is the refractive index of water, γ is the critical angle of total reflection glass/air, τ_w is the transmission coefficient of the water/glass interfaces and α is the angle of incidence in water.

By means of Snell's law

$$n_w \sin \alpha = n_j \sin j = 1 : \sin i,$$

equation (2) may be transformed to

$$T_{dw} = \int_0^{\frac{\pi}{2}} \Theta \sec j \; \tfrac{1}{2}(\tau_{wp}(\alpha)^3 \, \tau_p(i) + \tau_{ws}(\alpha)^3 \, \tau_s(i)) \frac{\sin 2i \; di}{n_w^2}$$

If we have two filters the τ_w's should be raised to the 5th power.

The integrals have been calculated on a computer with $n_w = 1.34$ and $n_j = 1.53$. In the spectrograph we measured the transmission values for a ray of normal incidence, T_{na}. For one filter

$$T_{na} = \Theta \; \tfrac{1}{2}(\tau_p(0)^2 + \tau_s(0)^2).$$

If we want the maximum values of T_{na} and T_{da} for one filter to be equal, that is $T_{da} = T_{na} = 0.914$ (for $\Theta = 1$), then

the values of diffuse transmission T_{da} and T_{dw} will be in relative units as in Table 1. It may seem strange that T_{dw} is smaller than T_{da}, since the reflection losses in water are restricted almost entirely to one surface, while there are four or six surfaces of equal reflection in air. This is due to the width of the light cone that the photocell receives from the opal glass, which is smaller in water than in air, and this compensates for the smaller reflection losses. However, no account is taken here of the radiance which may be greater and give greater photocurrent when there is water between the surfaces. Our results only concerns the transmitted irradiance. Any constant relative changes in sensitivity will be embodied in the immersion effect to be treated in the next chapter. We may therefore put $T_{dw}(\Theta=1) = 0.914$ for one filter, and we get the relative T_{dw}^*-values in Table 1.

The transmission curves (T_{na}) of the filter combinations are shown in fig. 2. Compared with Table 1(T_{da}), the errors introduced by diffuse light seem considerable; the smallest error is for RG1-RG5 (about 1%) and the greatest error for BG12+GG5 (about 15%). Due to our definition of the T_{dw}^*-values, there is good agreement between T_{da} and T_{dw}^* for one filter, but for the two-filter combination the distortion will be about 10%.

The errors become less if we take the reaction of the selenium cell to oblique, polarized rays into consideration. The functions $S_p(i)$ and $S_s(i)$ which are the sensitivity of the cell to the two components of transmitted light, are taken from Bergmann (1932, p.17-19) (see fig. 3). The relative photocurrent in air with one

filter is given by

$$P_a = \int_0^{\frac{\pi}{2}} \Theta \sec j \; \tfrac{1}{2}(\tau_p{}^4 S_p + \tau_s{}^4 S_s) \sin 2 i \, di,$$

and similar expressions are obtained for the other relative photocurrents. If we take the computed photocurrent to be a measure of the transmission, we get the relative values in Table 2. $P_w{}^*$ is defined in the same way as $T_{dw}{}^*$.

According to Teichmann (1932, p. 665-669) the functions $S_p(i)$ and $S_s(i)$ depend upon wavelength, which affects the reliability of Table 2. Table 1 and 2 were calculated under the assumption that the radiance from the opal glass is isotropic, an assumption that certainly is not correct. The real radiance distribution should give better coherence between T_d and T_{na}. Also it should be noted that the calculations were made for the center of the cell. Towards the edge of the cell the irradiance and the transmission errors decrease, while the sensitivity usually increases (Lange, 1940, p. 75), and what the result of these combined effects will be is difficult to estimate.

However, in the spectral calibration we use the T_{na}-values, and together with the known spectral irradiance distribution from a standard lamp, we try to find a sensitivity-function $S(\lambda)$ so that the equation

$$\int_{\lambda 1}^{\lambda_2} S(\lambda) \cdot T(\lambda)_f \cdot E_\lambda(\lambda) d\lambda = P_f$$

is satisfied for all filters (fig. 4). Here, the wavelengths λ_1 and λ_2 are the limits of transmission,

$E_\lambda(\lambda)$ ($= \frac{dE(\lambda)}{d\lambda}$) is the irradiance per unit wavelength and P_f is the read photocurrent for the filter combination. When we subsequently measure an unknown irradiance, we use the combined quantity $S(\lambda) \cdot T_{na}(\lambda)$ (curve 2-5 in fig. 4), which in fact should be independent of the filter transmission and only a function of the photocurrent and the irradiance of calibration. This may be seen from

$$S(\lambda) \cdot T_{na}(\lambda) = \frac{dp}{d\lambda} \quad \frac{1}{E_\lambda(\lambda)} \quad .$$

In this way there is a possibility that errors in the transmission cancel out.

The whole problem could be avoided by calibrating the spectral sensitivity of the irradiance meter for discrete wavelengths of known irradiance with the cell and filters as a unit. Unfortunately one usually has to use a light source with a continuous spectrum. The results in fig. 4 should then be regarded only as mean values in which finer details are lost. This also applies to the spectral irradiance distributions we obtain with this instrument.

The immersion effect

When the glass filters are submerged in water, their transmission increases because the reflection losses in water are smaller than in air. (The transmission discussed in the preceding chapter was the combined transmission of filters and window). The opal glass, however, will have less transmission in water. This is the immersion effect. The phenomena was given an explanation by Atkins and Poole in 1933 (p.135-139), and it has also been discussed by Jerlov (1951, p.14, 1966, p.14), Berger (1961, p.224) and Wes lak (1965, p.862-865).

The explanation by Atkins and Poole may be summed up as follows: Some of the light that penetrates into the opal glass and strikes the small, white particles that are dissolved in the glass, is scattered back towards the glass/air interface. If the angle of incidence exceeds ca. 41^{o}, the light undergoes total reflection. In water, however, the critical angle is ca. 63^{o}, which means that most of the light in the range $41\text{-}63^{o}$ is lost.

On the under side of the opal glass the same phenomena should give greater transmission, and a combination of the two effects is likely to give a number greater or smaller that 1, expressing the ratio of transmission in water to transmission in air. Still, empirically, the transmission always decreases by immersion.

Atkins and Poole did not experience the last of the above mentioned effects since they always had water between the opal glass and the window. They then found that

the sensitivity of the instrument was reduced to 82% in water for light of normal incidence. Unfortunately they assumed the radiance of natural light to be isotropic, and made corrections for this. The assumption is indeed wrong, but in this way they obtained the number 1.09 for the ratio of sensitivity in air to that in water. The number has later been referred to by several authors.

Berger, Jerlov and Westlake found that the sensitivity in water reduced to 78%, 82-88% and 78% respectively. In each case there was water between the opal glass and the window.

The spectral calibration of our instrument was performed in air with dry opal glass and filters to simplify the calibration. The glass surfaces were therefore dry in air in the following investigation of the immersion effect. The ratio of sensitivity in water to sensitivity in air will be called the immersion coefficient K. It varies with the filter combinations, which indicates that it is a function of wavelength.

Our method to determine the coefficient K requires that all the rays from the light source that hit the opal glass surface have small angles of incidence ($\cos i \approx 1$).

Let the light source be a point source and its intensity I. If the radius of the opal glass is a, and the distance to the light source H (fig. 5a), then in air the instrument receives the flux

$$F_a = I \, d\Omega_a = I \, \frac{\pi a^2}{H^2}$$

where $d\Omega_a$ is the solid angle in air from the light source to the opal glass. If there is water of depth z over the instrument (fig. 5b), the instrument receives the flux

$$F_w = I\, d\Omega_w\, \tau\, e^{-\kappa z}$$

$$= I\, \frac{\pi((H-z)\mathrm{tg}\ i)^2}{(H-z)^2}\, \tau\, e^{-\kappa z}$$

$$= I\, \pi\, \mathrm{tg}^2 i\, \tau\, e^{-\kappa z} \qquad (3)$$

Here, τ is the transmission coefficient air/water, and κ is the vertical attenuation coefficient for the light in water. We see from fig. 5b that

$$a = z\ \mathrm{tg}\ j + (H-z)\mathrm{tg}\ i \approx z\, \frac{\mathrm{tg}\ i}{n} + (H-z)\mathrm{tg}\ i,$$

where n is the refractive index of water.
This makes

$$\mathrm{tg}\ i = \frac{a}{H-(1-\frac{1}{n})z},$$

which, in view of (3), yields

$$F_w = I\, \pi\, \frac{a^2}{(H-(1-\frac{1}{n})z)^2}\, \tau e^{-\kappa z}$$

The ratio between the photocurrents p in the two media will then be

$$\frac{p_w}{p_a} = \frac{K \cdot F_w}{F_a} = K\, \frac{H^2}{(H-(1-\frac{1}{n})z)^2}\, \tau\, e^{-\kappa z}$$

K is the immersion coefficient defined earlier.

We can write

$$K = \frac{1}{\tau} \frac{p_w}{p_a} \left(1-\left(1- \frac{1}{n}\right) \frac{z}{H}\right)^2 e^{\kappa z}$$

Fresnel's laws give, for unpolarized light

$$\frac{1}{\tau} = \frac{(n+1)^2}{4\ n}$$

The variation of the refractive index with wavelength may be neglected, and by setting n = 1.34, we get

$$K = 1.022 \frac{p_w}{p_a} \left(1 - 0.254 \frac{z}{H}\right)^2 e^{\kappa z} \qquad (4)$$

This relation between K and the observed currents and depths was obtained for a point source. But since an extended light source may be regarded as several point sources, the formula applies also to this case, provided the angles of incidence remain small.

The centres of gravity, λg, for the filters are defined by

$$\int_{\lambda_1}^{\lambda g} T_{na}(\lambda)d\lambda = \int_{\lambda g}^{\lambda_2} T_{na}(\lambda)d\lambda$$

These are given for the filter combinations in Table 3, together with the values of κ and $e^{\kappa z}$ for z = 20 cm at the corresponding wavelengths. Whether one uses the attenuation coefficient for pure water (Clarke and James, 1939, p. 52)

or the vertical attenuation coefficient for the clearest ocean water (Jerlov, 1951, p.51), makes no difference at these small depths.

Several series of measurements were taken, but only the last three are presented here. In Series 1 the light source was a voltage-stabilized Philips sun lamp rated at 300 watts. The shielded lamp was mounted in the ceiling, and a plastic bucket with upper diameter 27 cm and height 30 cm was placed directly under the lamp. The irradiance meter, free from dust, was placed in the bucket, so that the opal glass was normal to the incident light. The distance between the opal glass and the front of the lamp was 2.53 m. First, the photocurrents were measured for all the filter combinations in air. Then the bucket was filled with distilled water until the opal glass was covered, and care was taken to remove air bubbles that were trapped between the filters. The photocurrent was read for different heights of water up to ca. 20 cm over the opal glass, and the readings were afterwards corrected for reflection from the walls of the bucket. The results are presented in fig. 6.

The curves have a bend from the surface down to 4-5 cm's depth below which K is constant. This is in agreement with the fact that the greatest depth z_o where light from the opal glass may undergo total reflection at the surface and hit the opal glass again, is

$$z_o = a/tg\gamma,$$

where a is the radius of the opal glass and γ is the

critical angle of total reflection (Atkins and Poole 1933, p.136, Berger, 1958, p.164). In our case, with 2 a = 8.5 cm, z_o is 3.8 cm.

The only exception to the description above is the value of RG5, which decreases all the way down. This indicates that the attenuation coefficient for this filter has been put too low.

To avoid possible reflection from the walls of the bucket, the inside was painted black, and the irradiance meter was placed on a platform with the opal glass 6 cm under the surface of the filled bucket. Series 2 was taken with this arrangement. The measurements in water were now reduced to one depth (6cm).

Series 3 was taken under the same conditions as Series 2, with the difference that the sun lamp was replaced by a 100 watt incandescent lamp, and the height H was reduced to 97 cm.

The results from Series 2 and 3, and the mean values of Series 1(6-20 cm) are presented in Table 4. The RG 5 values have been corrected for the attenuation seen on fig. 6. The employed values are shown in the column to the right.

The reason why the values of RG 1 and RG 5 are so high when the incandescent lamp is used, may be that its spectrum has the highest values in the red part, and that the immersion coefficient increases towards red. What we measure is an integrated immersion coefficient for each filter, while the results indicate that the coefficient

is a continous function of the wavelength. This view is confirmed by data presented by Smith and Tyler (1968). Fig. 7 shows our observed K-values for the instrument with opal glass and different filter combinations. As was said in the previous chapter, the way the immersion coefficient is defined here, it also contains the change in filter transmission due to immersion. The dashed lines in fig. 7 are the assumed $K(\lambda)$-functions of the instrument with opal glass that may give rise to our observed values. The K_n-function is obtained by correcting for reflection changes in the filters, assuming normal rays, and the K_d-function is obtained in the same way by assuming the light to be diffuse (Table 1). The actual function for our case should lie somewhere between these. Smith and Tyler do not tell how their $K(\lambda)$-function is derived, but when we compare it (solid line in fig. 7) with our results, we find the same tendency of wavelength-dependence. This means that the sensitivity function $S(\lambda)$ of the instrument has a shape in water different from that in air. For filters with broad transmission bands like ours, the immersion coefficient will vary somewhat with the spectral distribution of the irradiance, that is, it will change with depth in the ocean.

If the instrument is spectral-calibrated in a submerged state, this problem is avoided, and furthermore, as shown in Table 1 and 2, there will be greater resemblance between the normal and diffuse transmission values of the two-filter combinations (since the transmission do not exceed 40%).

Practical problems at sea.

For ideal measurements one requires

1: that the stations are taken while the light conditions in the sea are constant, and

2: that the observations give a true picture of the conditions.

Environmental factors which modify the results are, for point 1:

a. clouds which change the radiance distribution,

b. sun elevation which varies significantly during the observation period,

c. sea roughness which changes (important for low sun elevations,

and for point 2:

a. waves and rolling of the ship which lead to erroneous depths of recording,

b. currents which tilt the instrument and lead to erroneous depths of recording due to the wire-angle,

c. the relative position of the ship with respect to the instrument which can shade or irradiate with reflected light.

Three factors to be mentioned here are the change in radiance distribution, the wrong depth that arises from waves and ship rolling, and the shadow of the ship.

The first factor appears as a change in the reading of the sea photometer and the deck photometer.

Unfortunately there is no linear connection between the two readings, which makes it difficult to relate the data to a constant deck value. For 51 of 56 readings with the sea photometer at constant depth, and with the maximum/minimum value equal to 5:1, the deviations from linearity were $\leq$ 20%. The last five readings had deviations $\leq$ 70%. Still, the assumption of linearity is the only method we have so far to correct for sudden irradiance changes.

In a rough sea the uncertainty of the depth may be $\pm$ 1 m, which, e.g., corresponds to $\pm$ 30% of the RG1-RG5 reading. The uncertainty is to some degree corrected for by using that value in the region of uncertainty which seems most "reasonable", but in this way finer details are of course lost.

The errors in the readings introduced by the shadow of the ship, depend upon the radiance distribution and the solid angle from the instrument to the ship. Calculations on the dimensions of R/V Johan Hjort and radiance data from between 0 and 50 m (from Tyler, 1960), indicates that the errors in clear weather with sun and instrument on the same side of the ship, are less than 10%, while the errors in cloudy weather may amount to 20%, dependent on depth. (These numbers are significantly higher than those estimated by Poole in 1936 for the parallel case). No special corrections have been made for this, but some of the error may be regarded as eliminated by the depth-correction mentioned above. The effect of reflected light from the ship is more difficult to estimate.

The stations.

The four stations presented here were taken onboard R/V Johan Hjort and R/V G.O. Sars in march 1967 and April 1968, as a part of the IBP-project of Fiskeridirektoratets havforskningsinstitutt, Bergen. Table 5 gives the data of the stations and the locations are shown on fig. 8. The weather conditions given in Table 5 suggest changing light conditions, yet the variations in the deck readings were not great. For St. 1-4 the ratio of the largest to the smallest deck reading was 1.19, 1.14, 1.29 and 1.23, respectively.

Hydrographical data exist only for the two last stations, and their results showing two fairly homogeneous water masses (:Coastal water) are supported by the optical data in figs. 23, 24, 28 and 29. St. 1 and 2 show the same homogeneity in optical properties. The somewhat stronger attenuation for all wavelengths between 0 and 20 m on St. 4, may be due to greater biological activity in this region, and the strong attenuation in blue between 1 and 2 m on St. 2, may arise from yellow substance derived from a sewage-supply from ashore.

The irradiance distributions of St. 3 and 4 show a peculiarity in the upper layers. At 1 and 2 m depth St. 3 has two maxima at respectively 485 and 615 nm, and a strongly marked minimum at 565 nm. The vertical attenuation on figs. 23 and 24 indicates that the readings are right, and the same tendencies are found also at St. 4. If there

are no errors in the observations, then the irregularities are probably due to some absorption or scattering phenomena in the atmosphere.

The irradiance maxima at the greatest depths of St. 1 and 4 occur at 495 nm, while at St. 2 and 3 they occur at 515 and 510 nm, which means that the water at St. 1 and 4 is more blue than at St. 2 and 3. Since the clearest water is the most blue, it is to be expected that the least vertical attenuation occurs at St. 1 and 4. Figs. 9a and b confirm this rule. The figures also show the normal transmission curves for coastal water at 45° solar altitude (Jerlov, 1951, p. 50-51), and for ocean water at zenith sun. To relate the stations to a common solar altitude (45°), the data have been corrected for differences in mean path length according to Jerlov (1951, p. 42-43). (Only St. 4 had to be corrected).

Fig. 9b shows the vertical attenuation of the integrated irradiance in the range 340-740 nm. St. 1 appears to have a mean total transmission between ocean water II and III, St. 2 between coastal water 1 and ocean water III, St. 3 at about coastal water 1, and St. 4 between ocean water II and III. This is about what one should expect. According to Jerlov (1968, p. 123) the water in Skagerak is coastal water 1, and both unpublished and published data from Aarthun (1961) show that the waters below 10 m in the outer part of the Hardanger Fjord are coastal water 1 to ocean water III. As long as we lack data from the Norwegian Sea, further interpretations from our stations are futile.

The mean spectral transmissions shown in fig. 9a, prove clearly that the transmission values in the red part of the spectrum are too high; that is, the combination RG1-RG5 has a light-leakage in the green or blue (Tyler, 1959, p. 102). Better results should be obtained with 3 instead of 2 mm filter thickness. The transmissions at 350 and 375 nm may also be a bit too high. The contributions from these parts of the spectr m are of minor importance in the integrated irradiance, which is shown in absolute values on fig. 30. The surface values are obtained by extrapolating the spectral attenuation curves to the surface, a method which is apt to give too high values.

The irradiance data are also presented in digital form in Table 6-9.

Acknowledgements.

The author gives due thanks to Universitetets Institut for Fysisk Oceanografi, Copenhagen, Institutt for marin biologi, Institutt for kosmisk fysikk, Oslo, and Fiskeridirektoratets havforskningsinstitutt, Bergen, for theoretical, instrumental and practical support.

REFERENCES

Atkins, W.R.G. and Poole, H.H., 1933. The Photo-Electric Measurement of the Penetration of Light of various Wave-Lengths into the Sea and the Physiological Bearing of the Results. Phil.Trans.Roy.Soc. vol.222-B.

Berger, F., 1958. Über die Ursache des "Oberflächen-effekts" bei Lichtmessungen unter Wasser. Wetter und Leben, 10.

Berger, F., 1961. Über den "Taucheffekt" bei der Lichtmessungen über und unter Wasser. Arch.Meteor.Geoph.Biokl.Serie B, Band II, 2. Heft.

Bergmann, L., 1932. Über die Einwirkung von polarisierten Licht auf Sperrschicht-Photozellen. Physik.Zeitschr., 33.

Clarke, G.L. and James, H.R., 1939. Laboratory analysis of the selective absorption of light by sea water. J.Opt.Soc. A, 29.

Jerlov, N.G., 1951. Reports of the Swedish Deep-Sea Expedition. vol. III, Physics and Chemistry. No. 1. Göteborgs Kngl.vetensk. vitterh. samh.

Jerlov, N.G., 1968. Optical Oceanography, Elsevier Publishing Company.

Lange, B., 1940. Die Photoelemente und ihre Anwendung. Johann Ambrosius Barth, Verlag, Leipzig, Bind I-II. 2 Auflage.

Petterson, H. and Poole, H.H., 1937. Measurements of submarine Daylight. Göteborgs kngl.vetensk.vitterh.samh.

Poole, H.H., 1936. The photo-electric measurement of submarine illumination in off-shore waters. Rapp.Conseil Perm. Inter.Expl. Mer.,vol. 101, 2,2.

Smith, R.C. and Tyler, J.E., 1968. Spectral Irradiance Data. Scripps.Inst.Oceanog., Vis.Lab., Calif., Ref 68-29.

Teichmann, H., 1932. Das elektrische Verhalten von Grenzschichten. Ann.Physik, 13.

Tyler, J.E., 1959. Natural Water as a Monochromator. Limn. Oceanogr., 4.

Tyler, J.E., 1960. Radiance distribution as a function of depth in an underwater environment. Bull.Scripps. Inst. Ocean. Univ. Calif., 7.

Westlake, D.F., 1965. Some Problems in the Measurement of Radiation under Water: A Review. Photochem. Photobiol., vol. 4.

Aarthun, K.E., 1961. Submarine daylight in a glacier-fed Norwegian fjord. Sarsia 1.

Table 1

	1 filter			2 filters		
T_{na} %	T_{da} %	T_{dw} %	T_{dw}^* %	T_{da} %	T_{dw} %	T_{dw}^* %
10	7.78	5.18	7.62	7.75	5.67	8.35
20	16.8	11.2	16.5	16.7	12.3	18.1
30	26.3	17.7	26.1	26.2	19.4	28.5
40	36.3	24.5	36.0	36.1	26.8	39.4
50	46.5	31.4	47.0	46.2	34.4	50.7
60	57.1	38.6	56.8	56.7	42.3	62.3
70	67.8	45.9	67.6	67.3	50.3	74.1
80	78.7	53.4	78.6	78.1	58.5	86.2
90	89.8	61.0	89.8			

Table 2

	1 filter		2 filters	
T_{na} %	Pa %	Pw^* %	Pa %	Pw^* %
10	8.27	8.24	8.40	9.00
20	17.5	17.5	17.8	19.1
30	27.2	27.1	27.6	29.7
40	37.2	37.1	37.7	40.6
50	47.4	47.3	48.1	51.8
60	57.8	57.7	58.7	63.1
70	68.3	68.3	69.4	74.7
80	79.0	79.0	80.3	86.4
90	89.9	89.9		

Table 3

Filter	λg nm	κ m^{-1}	$e^{\kappa} \cdot 0{,}2$ m
UG1 + BG12	380	0.0353	1.007
BG12 + GG5	470	0.0176	1.003
VG9	520	0.0372	1.008
RG1	620	0.274	1.056
RG5	670	0.401	1.083

Table 4

Filter	Sun lamp		Incandescent lamp	Employed
	$\bar{K}$(Series 1)	K(Series 2)	K(Series 3)	K
BG1 + BG12	0.724	0.721	Unmeasureable	0.722
BG12 + GG5	0.672	0.675	0.674	0.674
VG9	0.653	0.668	0.669	0.669
RG1	0.685	0.684	0.726	0.690
RG5	0.71	0.71	0.76	0.690

Table 5

	Position	Date	Local time	Solar altitude
St.1	62.5°N 6.0°E	14/3-67	1330 - 1430	24.5° - 22.1°
St.2	62.4°N 6.1°E	15/3-67	1000 - 1100	18.3° - 22.5°
St.3	63.3°N 7.9°E	20/4-68	1200 - 12.50	38.0° - 38.1°
St.4	65.8°N 10.5°E	23/4-68	12.25 - 13.25	25.3° - 24.8°

	Cloud cover	Wind *	Depth, m
St. 1	8/8, melting snow, drizzle	4	32
St. 2	8/8	1	44
St. 3	8/8, drizzle	2	215
St. 4	4/8, mist	2	310

* Beaufort scale

Table 6. Irradiance E_λ at St. 1

λ in nm, E_λ in mW m^{-2} nm^{-1}.

λ	0m	2m	5m	10m	20m	30m
340	22	7.8	1.6	0.28	0.0114	0.00044
5	24.5	9.3	2.2	0.41	0.0189	0.00085
6	27	11.3	3.0	0.60	0.0328	0.0017
7	30	13.2	4.0	0.861	0.056	0.0034
8	32.5	15.7	5.1	1.29	0.095	0.0067
9	35.5	18.6	6.8	1.90	0.164	0.0134
400	38.5	21.5	8.9	2.70	0.29	0.0268
1	41	25.0	11.3	3.82	0.48	0.055
2	44	28.5	14.7	5.4	0.81	0.11
3	47	32.5	18.0	7.3	1.4	0.22
4	50	36.0	21.7	9.5	2.3	0.41
5	53	39.5	25.9	12.3	3.54	0.85
6	56	43	29.0	15.1	5.37	1.51
7	58.5	46	32.3	18.0	7.0	2.6
8	61.5	48.9	35.0	20.3	8.45	3.75
9	64	51	36.7	21.5	9.4	4.4
500	67	53	37.8	21.7	9.55	4.4
1	70.5	54.8	37.2	21	8.7	4.0
2	73.5	55.5	36.3	19.8	7.5	3.2
3	76.5	56	34.4	17.1	6.0	2.0
4	79	55.8	33	15.1	4.6	1.36
5	80	55	31	14.1	3.4	0.85
6	80	53.5	29	12.0	2.45	0.5
7	79	51.5	26.8	10.2	1.65	0.24
8	77	49	24.7	8.5	1.06	0.12
9	75	46	22.5	7.0	0.66	0.061
600	73	43.7	20.2	5.8	0.43	0.031
1	71	41.3	18.1	4.6	0.264	0.0164
2	69	39	16.3	3.6	0.169	0.0082
3	67	36.5	14.7	2.8	0.106	0.0041
4	65	34	12.9	2.1	0.066	0.0020
5	63	31.8	11.2	1.62	0.043	0.001
6	61	29.5	9.8	1.23	0.025	0.0005
7	59	27.0	8.5	0.9	0.0161	0
8	57	24.9	7.2	0.66	0.0103	
9	55	22.9	6.0	0.48	0.0066	
700	53	20.8	5.0	0.36	0.0043	
1	51.3	18.9	4.1	0.26	0.0026	
2	49.5	17.0	3.3	0.19	0.0017	
3	48	15.2	2.7	0.133	0.0011	
4	46.5	13.8	2.65	0.095	0.0007	

Table 7. Irradiance E_λ at St. 2

λ in nm, E_λ in mW m^{-2} nm^{-1}.

	0m	1m	2m	5m	10m	20m	30m	40m
340	8.1	2.4	0.667	0.11	0.01	0.0009	0.0001	
5	10.1	3.1	0.94	0.19	0.019	0.0015	0.00015	
6	12.8	4.1	1.33	0.32	0.033	0.0023	0.00024	
7	15.7	5.3	1.89	0.51	0.055	0.004	0.00038	
8	19.2	7.0	2.61	0.77	0.098	0.007	0.00068	
9	24	9.1	3.7	1.20	0.175	0.013	0.0012	
400	30	12.3	5.06	1.90	0.28	0.02	0.002	
1	36.5	16	7.0	2.9	0.47	0.04	0.005	
2	46	21	9.5	4.2	0.79	0.07	0.008	0.001
3	55.5	26.5	12.5	6.0	1.3	0.13	0.017	0.0017
4	67	33.7	16.2	8.5	2.04	0.24	0.034	0.004
5	79	42	21.3	11.0	3.25	0.45	0.069	0.011
6	90	50	27.0	14.8	5.1	0.79	0.15	0.027
7	101	58	33.4	18.5	7.3	1.45	0.32	0.062
8	110	67	41	22.6	10.2	2.33	0.69	0.16
9	117	76	50	26.6	13.0	3.73	1.37	0.40
500	123	84	58	30.6	16	5.7	2.86	1.01
1	130	90.5	65	34.5	18	6.9	3.60	1.53
2	135	96.5	70	37.5	19	7.3	3.70	1.45
3	140	101	74	40.0	19	7.0	3.1	0.82
4	142	104	77	40.8	18.5	6.4	2.3	0.31
5	142.3	105.5	78	40.0	17	5.0	1.1	0.11
6	141.3	105	77.5	38.5	15	3.6	0.55	0.042
7	139	102.5	76	35.5	13	2.5	0.25	0.016
8	135.5	99.2	74	32	11	1.6	0.12	0.006
9	131.5	96	71	28	9	0.95	0.071	0.0023
600	127.5	92.5	68	24	7.5	0.55	0.035	0.001
1	124	89	64.5	20.8	5.9	0.32	0.014	
2	121	83	60	17.0	4.8	0.20	0.007	
3	117.5	79.5	55	14.2	3.5	0.12	0.003	
4	114.5	74.5	50	11.9	2.8	0.075	0.0015	
5	111.5	70	44.5	9.6	2.1	0.046	0.001	
6	108.5	65	39.5	7.9	1.6	0.029		
7	105.5	60	35	6.4	1.2	0.017		
8	102	55.5	30.5	5.1	0.9	0.0105		
9	99.5	52	26.5	4.1	0.67	0.0065		
700	96	48	23.3	3.3	0.5	0.004		
1	93.5	44	20	2.7	0.38	0.0023		
2	90.5	40	17.5	2.18	0.28	0.0015		
3	87.5	36	15.0	1.7	0.21	0.0012		
4	85	33	13.0	1.4	0.16	0.001		

Table 8. Irradiance E_λ at St. 3

λ in nm, E_λ in mW m^{-2} nm^{-1}

λ	0m	1m	2m	5m	10m	20m	30m	40m	50m
340	23.5	17	12.0	4.16	0.75				
5	28	20.5	14.5	5.32	1.0				
6	34.5	24.5	17.2	6.77	1.37				
7	41	29.5	20.9	8.7	1.8				
8	49	35	24.5	10.6	2.4				
9	60	42	29	13.1	3.1				
400	70	49	34.5	15.5	4.0	0.33	0.024	0.00073	
1	80	57	41	19.5	5.0	0.47	0.043	0.00165	
2	90	65	48	23	6.25	0.66	0.072	0.0038	0.0002
3	100	74	55	27	7.7	0.95	0.121	0.0078	0.00065
4	110	82	62.5	31	9.3	1.3	0.197	0.0165	0.0018
5	120	91	70	36	11.0	1.8	0.295	0.035	0.0044
6	130	99	76	40	13.0	2.4	0.492	0.073	0.01
7	138	105	82.5	44	15.0	3.2	0.77	0.141	0.025
8	139	110	88	48	17.5	4.2	1.17	0.262	0.055
9	132	108	86	50.5	20.0	5.3	1.7	0.46	0.125
500	118	95	80	51	22.5	6.8	2.54	0.70	0.23
1	100	84	73	50	24.7	8.09	3.42	1.13	0.437
2	86	75	69	48	25.2	8.09	3.03	0.75	0.278
3	78	70	65	45.5	24	7.0	2.24	0.44	0.139
4	73	66.6	61	43	22	5.6	1.51	0.25	0.067
5	69	64	59	40	19.5	4.4	0.955	0.14	0.0307
6	68	62	57	37	16.5	3.34	0.538	0.074	0.0129
7	70	62	55.5	34	13.5	3.26	0.291	0.038	0.0054
8	77	65	55	31	10.8	1.4	0.146	0.0172	0.0024
9	86	69	57	28.5	8.5	0.86	0.073	0.0078	0.001
600	119	89	60	26	6.2	0.42	0.036	0.0039	0.00039
1	150	97.8	64	23	4.8	0.238	0.0178	0.00187	0.00017
2	150	97.8	65	21	3.4	0.134	0.009	0.00086	
3	142	94.7	62	18.5	2.5	0.067	0.0044		
4	135	88.5	59	16.0	1.7	0.036	0.0023		
5	128	82.4	54	13.5	1.15	0.019			
6	120	77.2	49	11.7	0.78	0.0105			
7	110	71	44	10.0	0.53				
8	103	64.3	40	8.5	0.33				
9	94	58.7	36	7.0	0.203				
700	85	53.5	33	5.9	0.124				
1	77	48.4	29	4.8	0.093				
2	70	44.3	26	4.0					
3	62	40.1	23.5	3.2					
4	55	36.0	21	2.6					

Table 9. Irradiance E_λ at St. 4

λ in nm, E_λ in mW m^{-2} nm^{-1}.

λ	0m	1m	2m	5m	10m	20m	30m	40m	50m
340	190	140	100	28	6.1	0.196	0.0159	0.0021	0.00028
5	235	170	125	38	8.8	0.33	0.031	0.0042	0.00068
6	280	205	150	50	12.1	0.57	0.059	0.0090	0.00181
7	330	245	180	69	16.7	0.98	0.116	0.0201	0.0045
8	380	290	215	89	23	1.65	0.243	0.045	0.0113
9	430	340	260	116	32	2.8	0.444	0.094	0.0271
400	490	390	305	150	45	4.5	0.82	0.198	0.055
1	540	440	360	182	60	7.0	1.45	0.34	0.097
2	590	500	420	230	80	11.0	2.48	0.65	0.194
3	640	550	470	270	110	17.0	4.1	1.20	0.387
4	695	600	520	320	140	26.0	6.7	2.10	0.73
5	745	650	570	370	175	38	11.4	3.72	1.45
6	800	700	620	420	215	54	18.1	6.8	2.9
7	845	750	660	470	250	71	28.9	12.4	5.3
8	890	800	710	510	272	86	41.3	22	9.87
9	930	830	740	540	300	96	46.5	26.5	14.8
500	960	860	774	559	308	101.5	46.6	25.9	15.2
1	960	860	774	559	298	97	43.6	19.9	10.4
2	940	850	774	539	271	88	35.5	12.9	5.5
3	920	840	754	508	244	69	25.3	7.5	2.76
4	900	810	723	468	212	50	14.7	4.2	1.23
5	875	780	703	427	175	31	8.0	2.0	0.512
6	850	750	672	386	138	18.6	4.1	0.9	0.205
7	840	720	621	325	106	10.9	2.0	0.38	0.077
8	850	700	581	274	80	6.2	1.0	0.15	0.0266
9	930	700	535	224	54	3,6	0.47	0.06	0.0092
600	1020	700	487	169	38	2.1	0.24	0.025	0.00204
1	1180	700	426	131	25	1.14	0.12	0.01	
2	1300	690	375	108	17	0.64	0.058		
3	1290	670	360	89	11.7	0.35	0.029		
4	1215	640	340	70	8.0	0.21	0.014		
5	1180	590	294	56	5.3	0.11	0.009		
6	1150	540	252	46	3.4	0.66	0.005		
7	1110	500	220	39	2.2	(0)			
8	1060	450	190	31	1.4				
9	1000	400	163	24	0.95				
700	930	360	140	19.5	0.65				
1	900	330	120	15.2	0.42				
2	860	290	100	12.0	0.28				
3	840	265	85	9.6	0.185				
4	800	235	72	7.8	0.12				

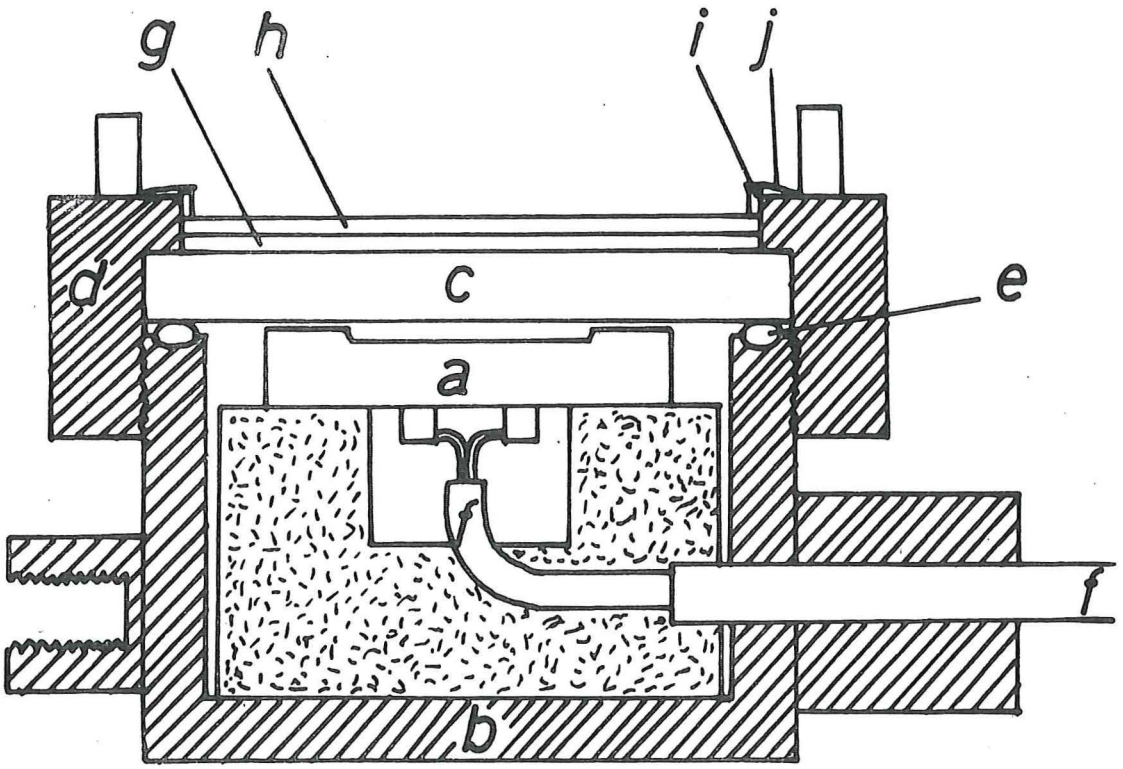

Fig. 1. The irradiance meter

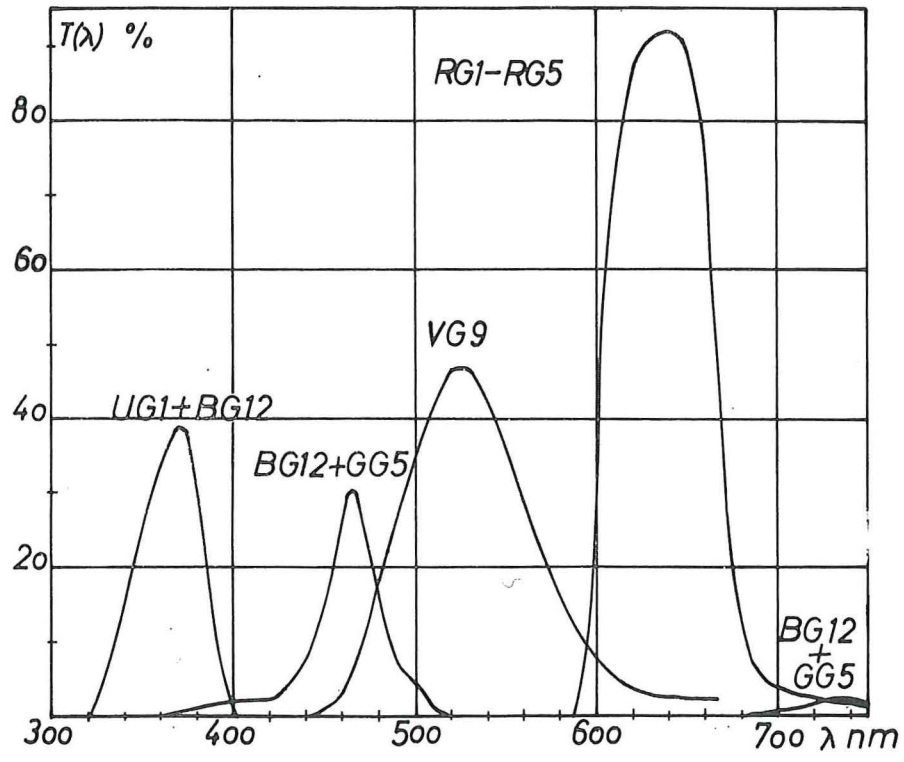

Fig. 2. Transmission curves (T_{na}) of the filters.

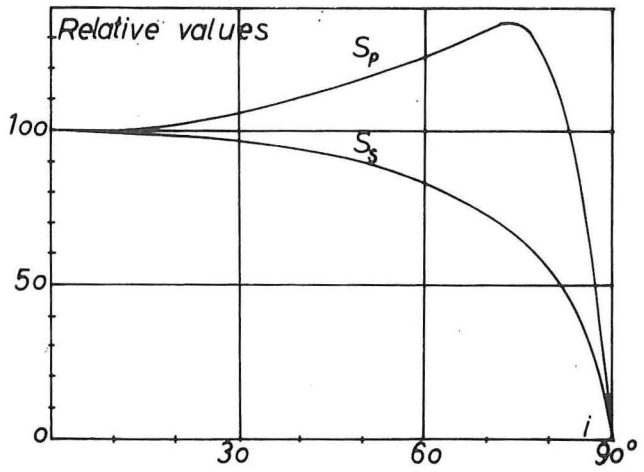

Fig. 3. The sensitivity functions $S_p(i)$ and $S_s(i)$ of the selenium cell. After Bergmann, 1932.

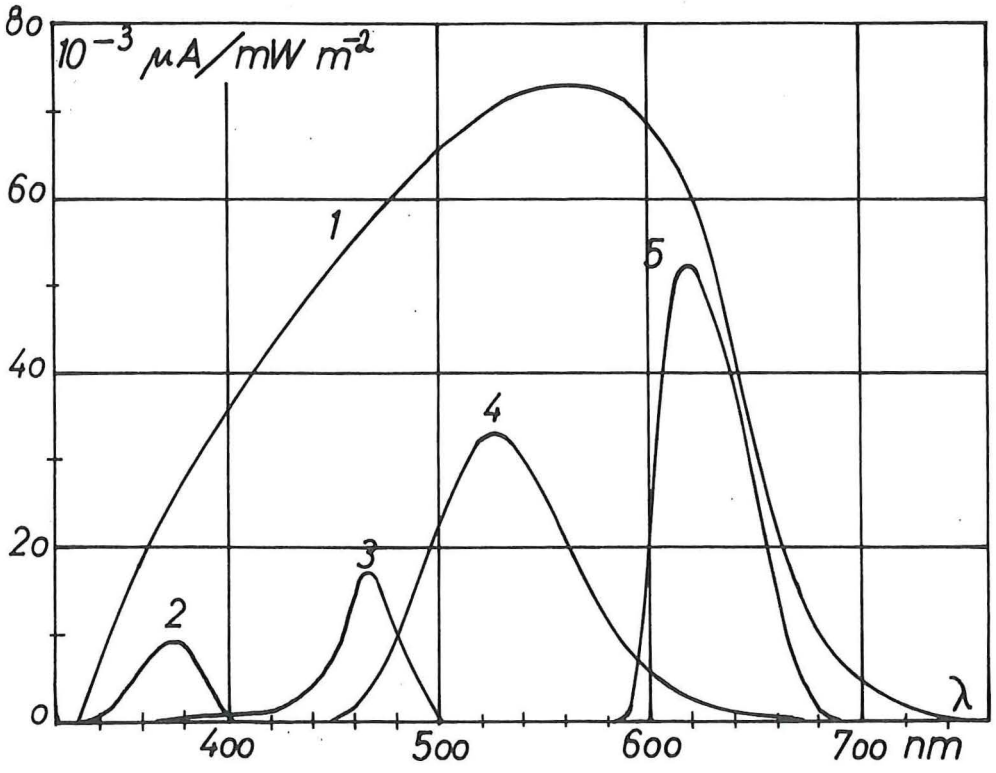

Fig. 4. Spectral sensitivity of the EEL-cell with
opal glass (Curve 1)
" and VG1 + BG12 (Curve 2)
" and BG12 + GG5 (Curve 3)
" and VG9 (Curve 4)
" and RG1 - RG5 (Curve 5)

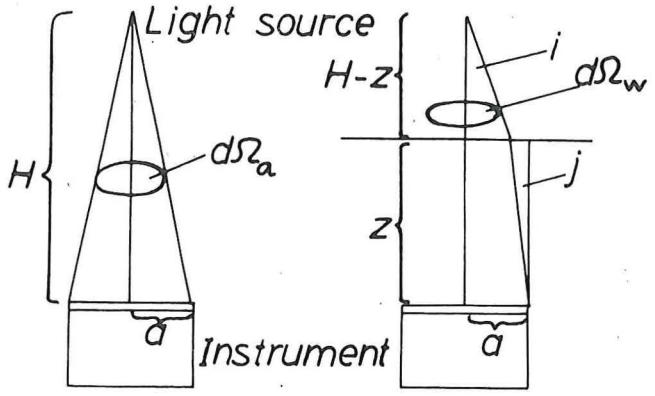

Fig.5a. Flux reaching the instrument in air.

Fig.5b. Flux reaching the instrument in water.

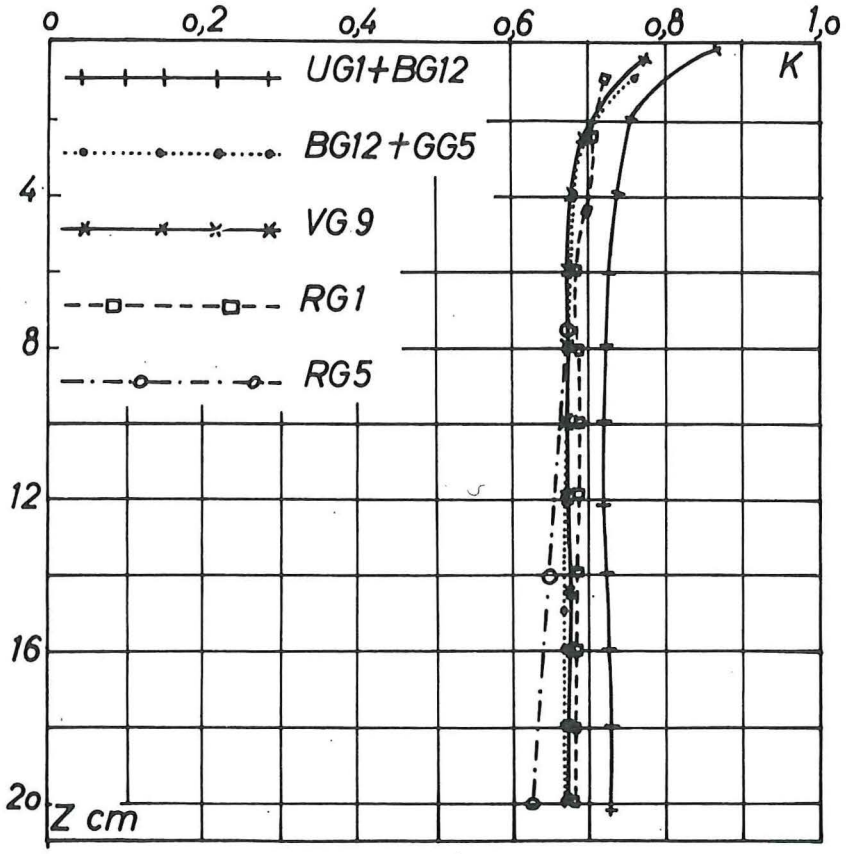

Fig. 6. The immersior coefficient K as a function of the depth z.

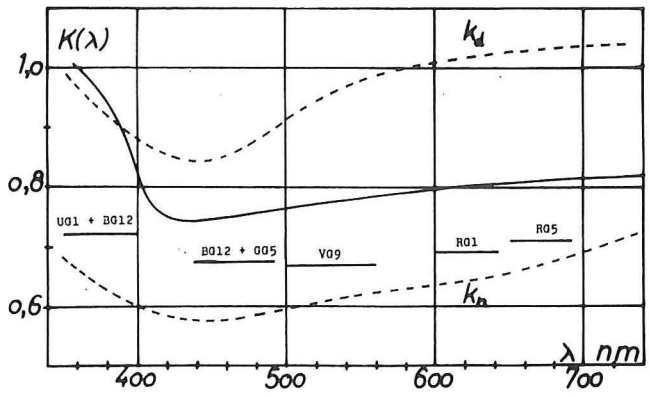

Fig. 7. The immersion coefficient K as a function of the wavelength λ.
Dashed lines: our results, solid line: Smith and Tyler, 1968.

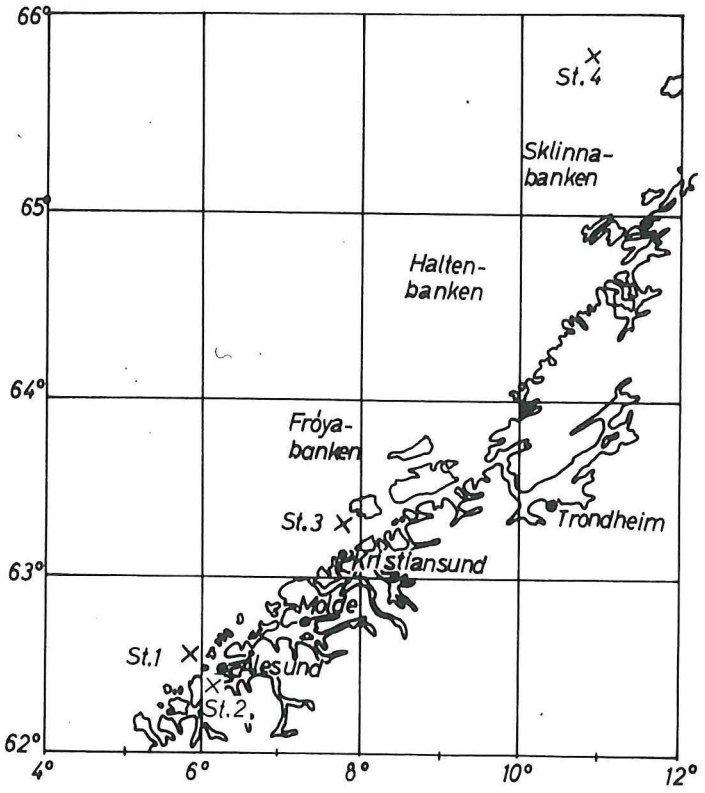

Fig. 8. Locations of the stations.

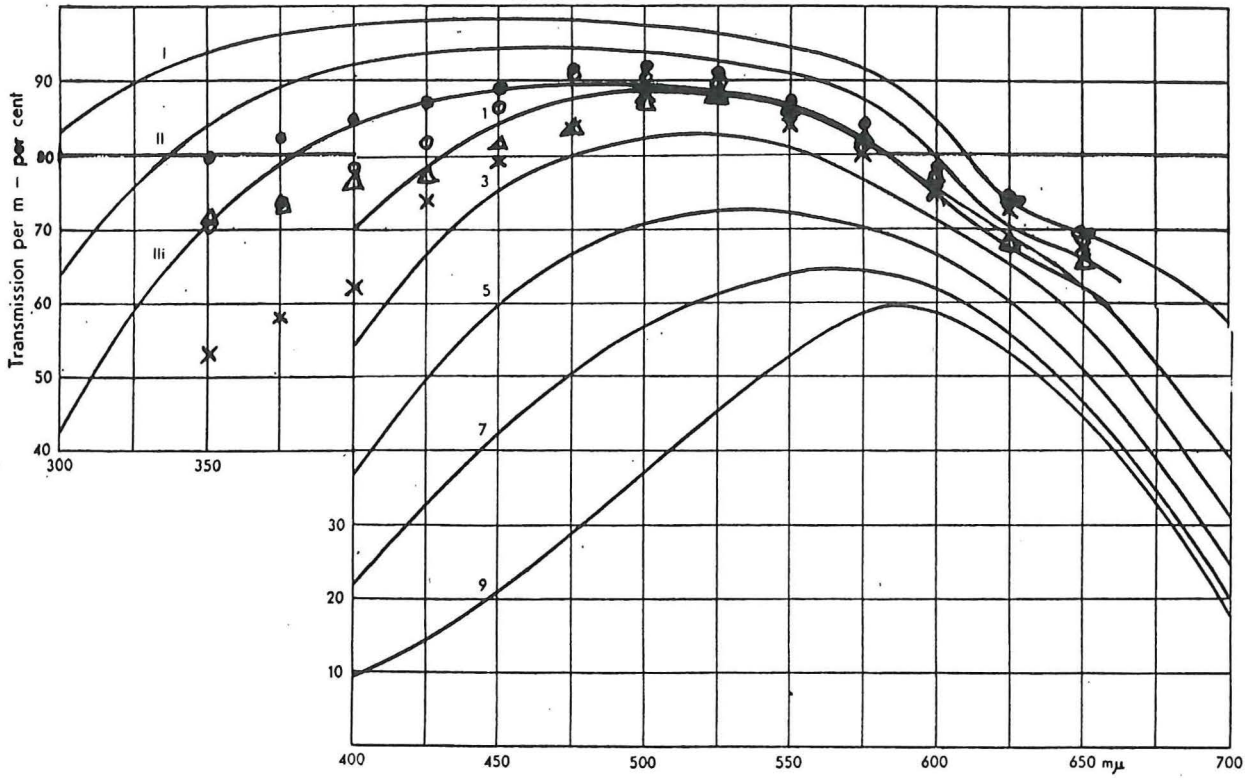

Fig. 9a. Normal transmission curves for coastal water at 45° solar altitude. (Curve 1-9), and for ocean water at zenith sun (Curve I-III). After Jerlov, 1951.

o St.1, X St.2, Δ St.3, • St.4.

Fig. 9b. Total transmission (340-740 nm) of the different water types. After Jerlov, 1968.

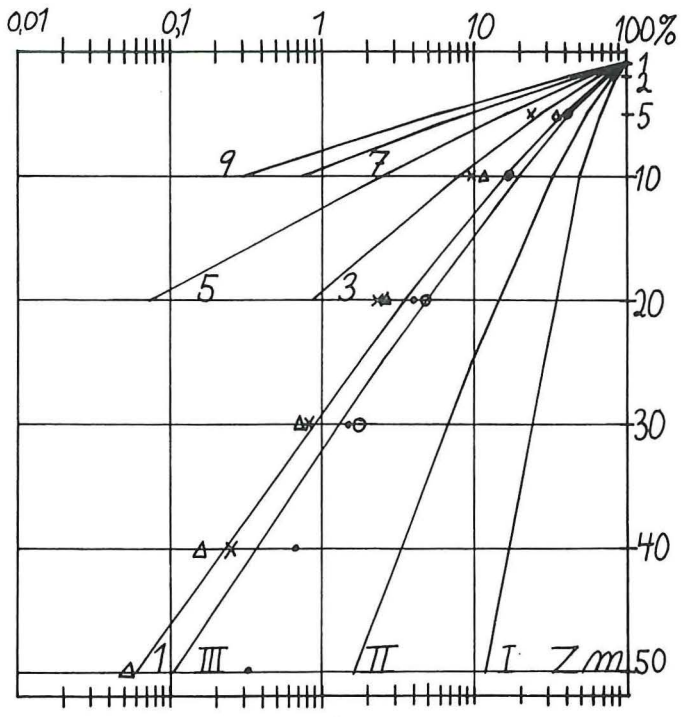

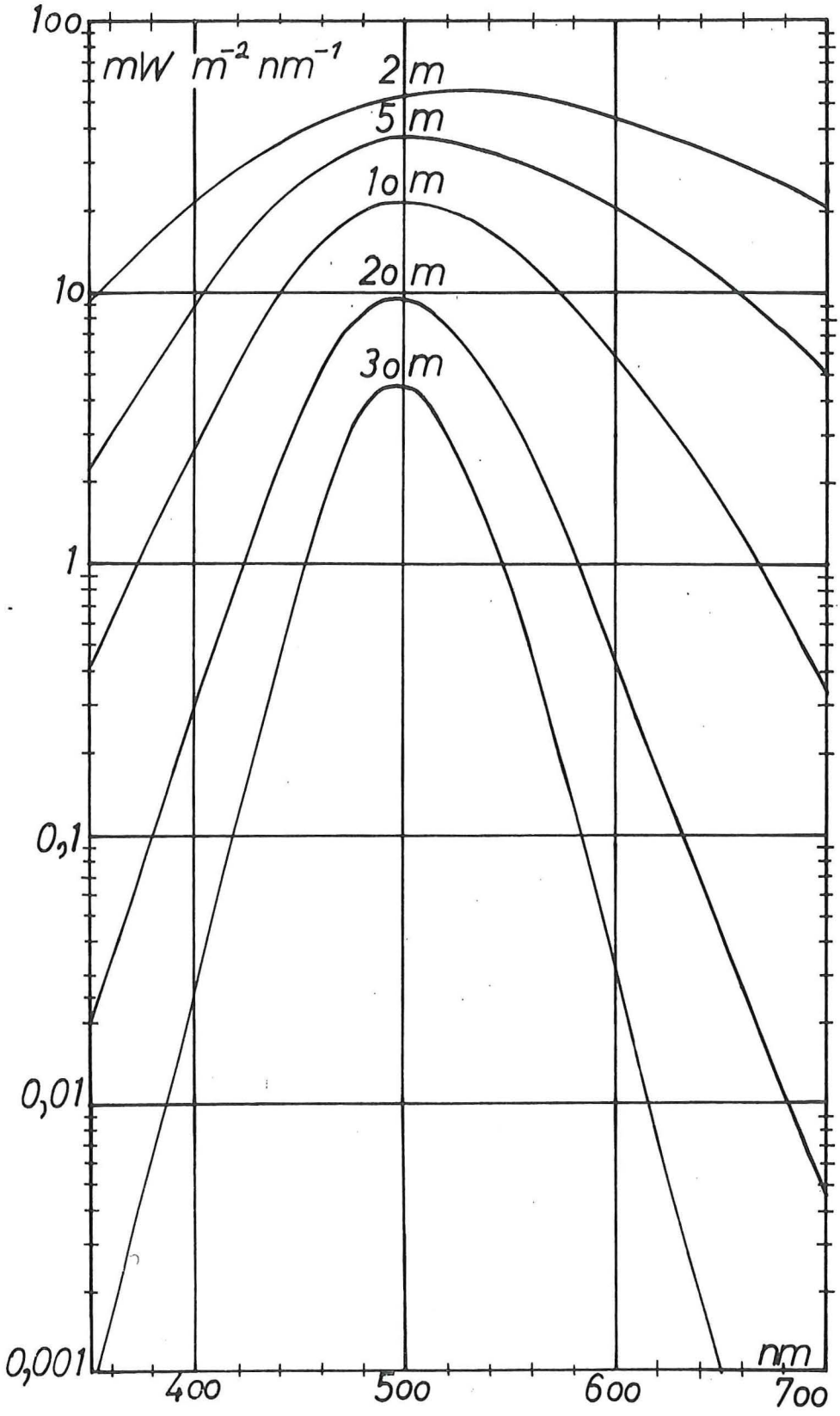

Fig. 10. St. 1. Irradiance.

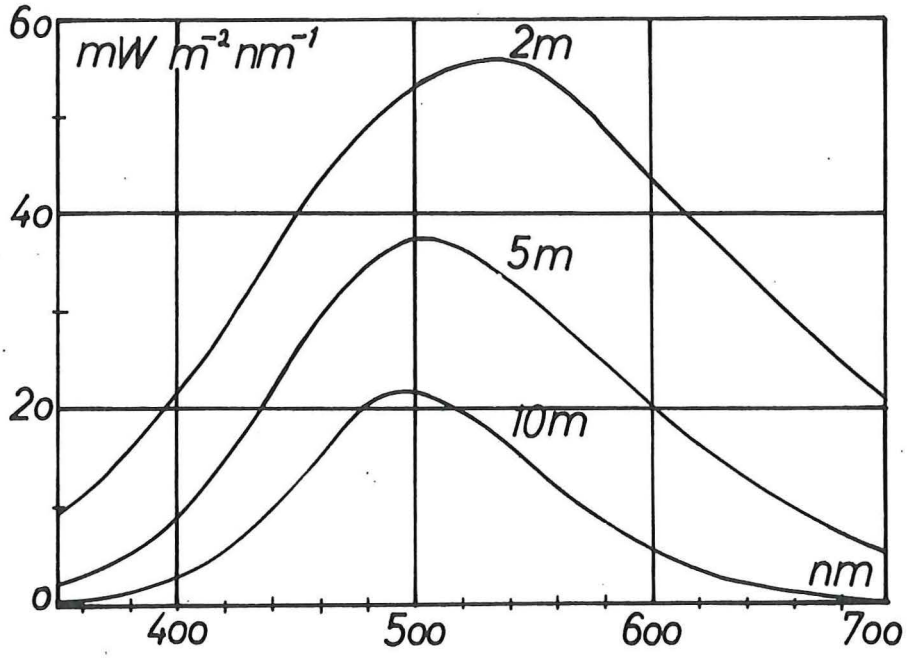

Fig. 11. St. 1. Irradiance.

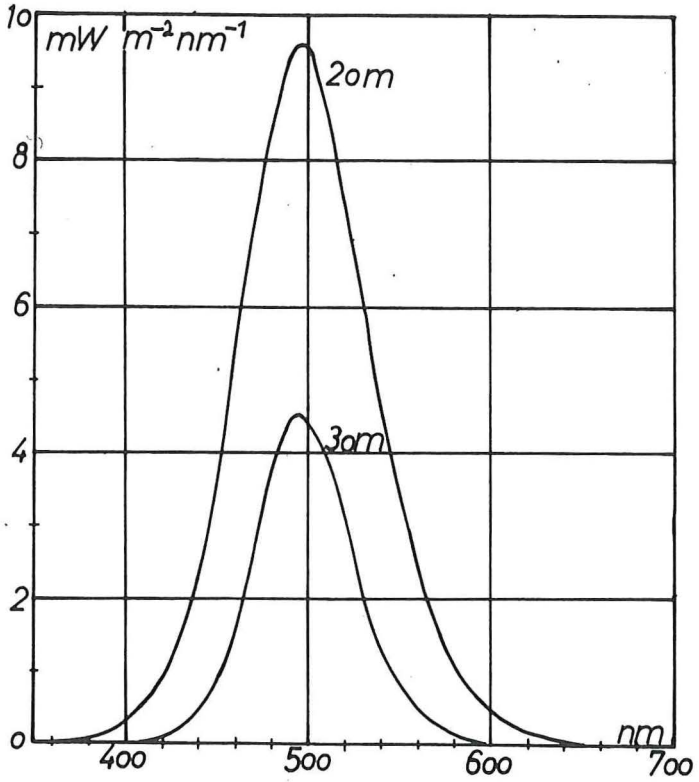

Fig. 12. St. 1. Irradiance.

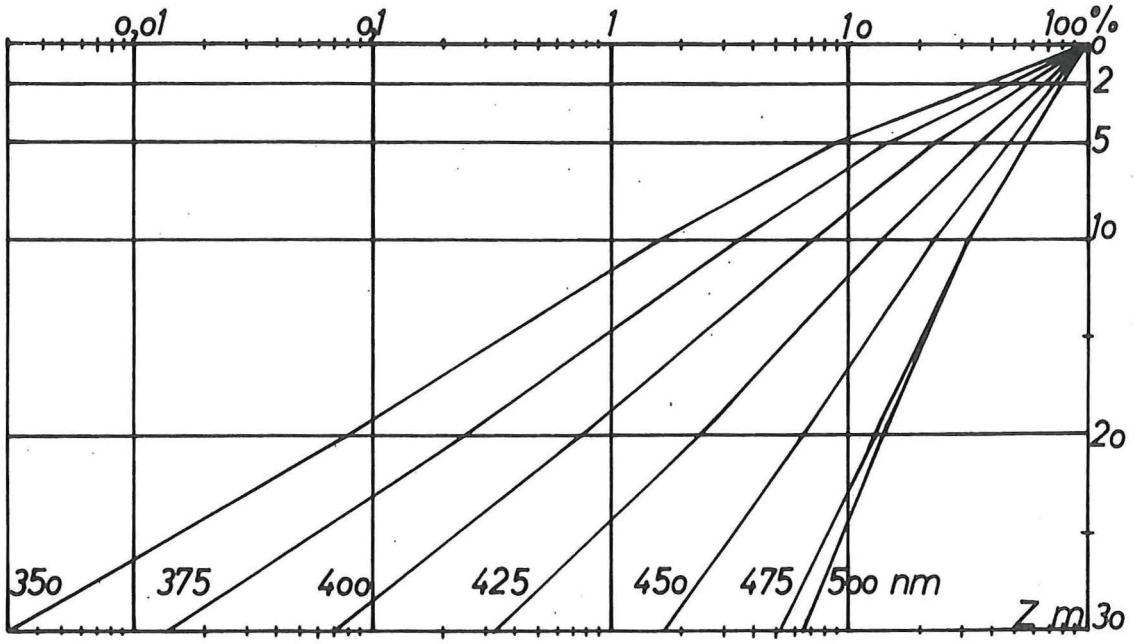

Fig. 13. St. 1. Vertical attenuation..

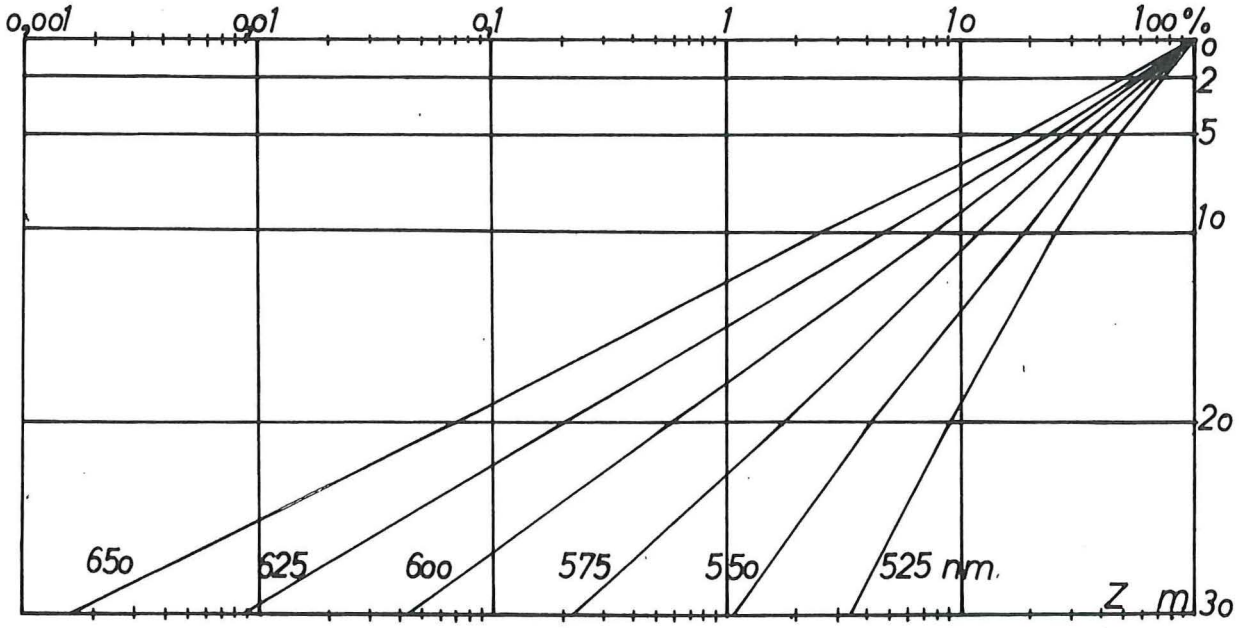

Fig. 14. St. 1. Vertical attenuation.

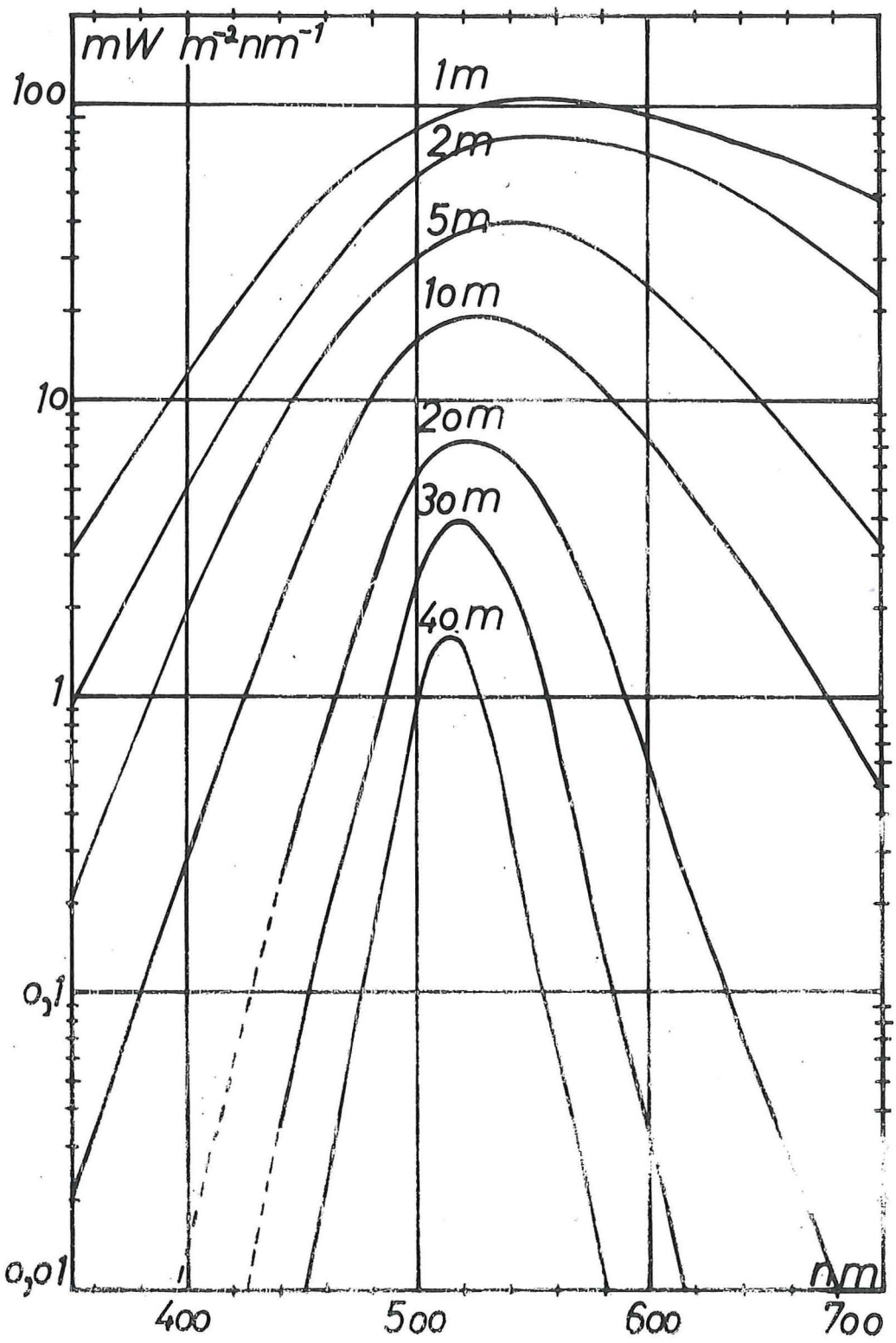

Fig. 15. St. 2. Irradiance.

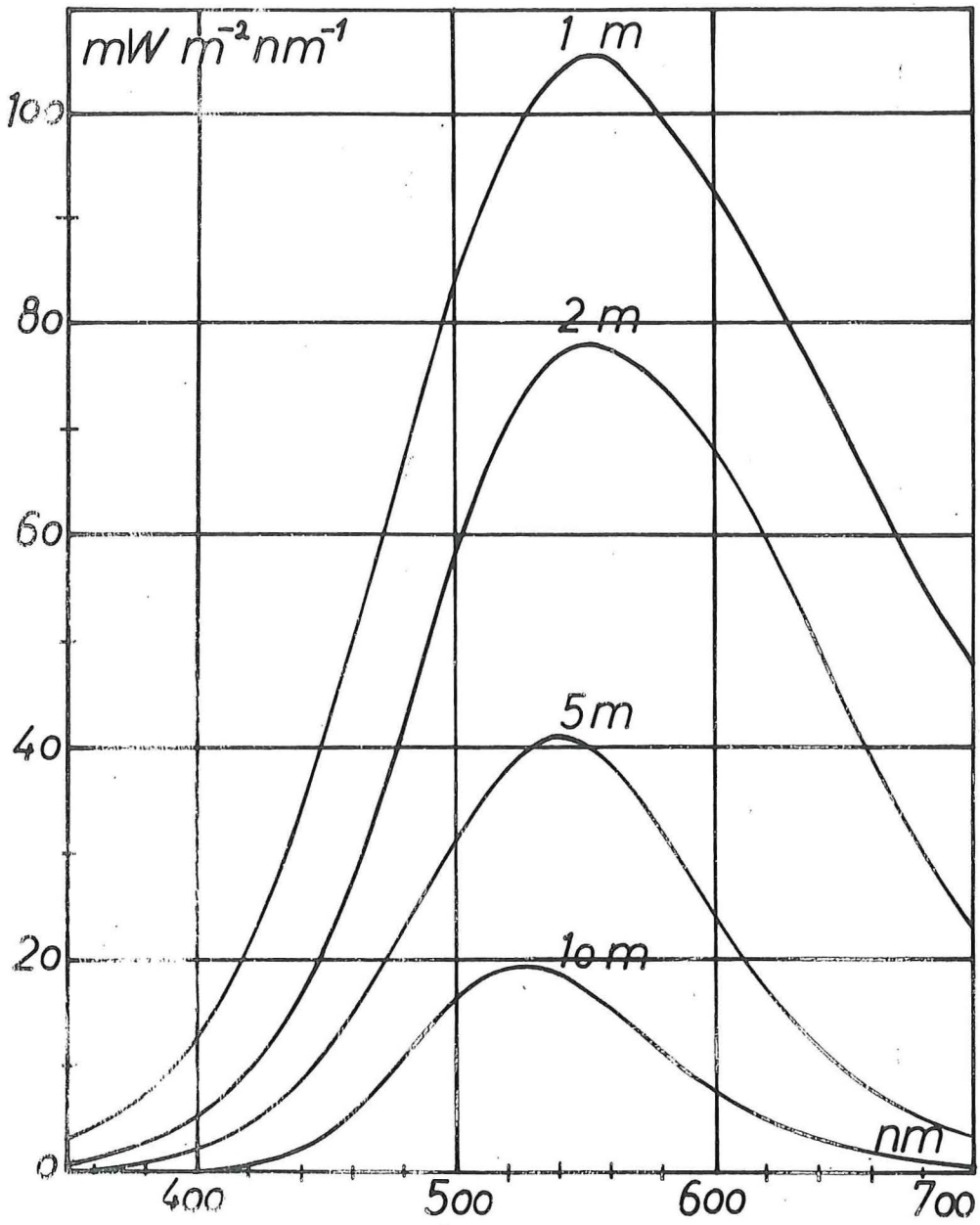

Fig. 16. St. 2. Irradiance.

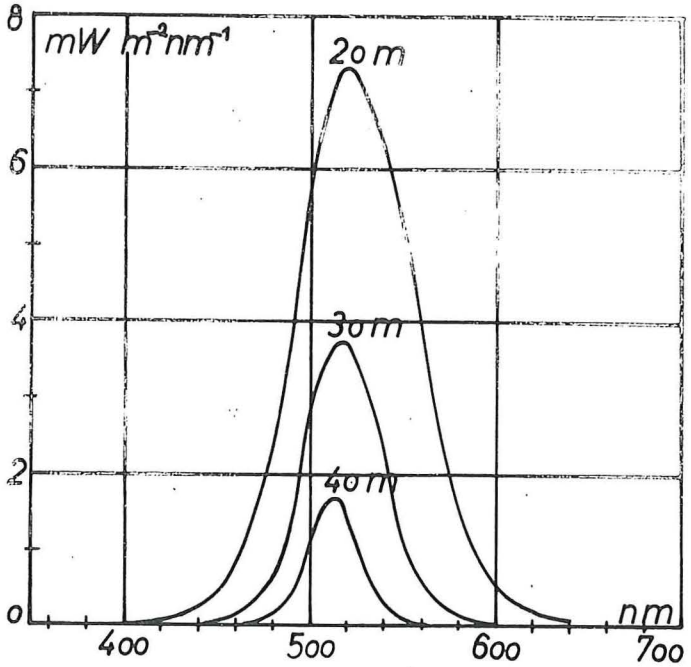

Fig. 17. St. 2. Irradiance.

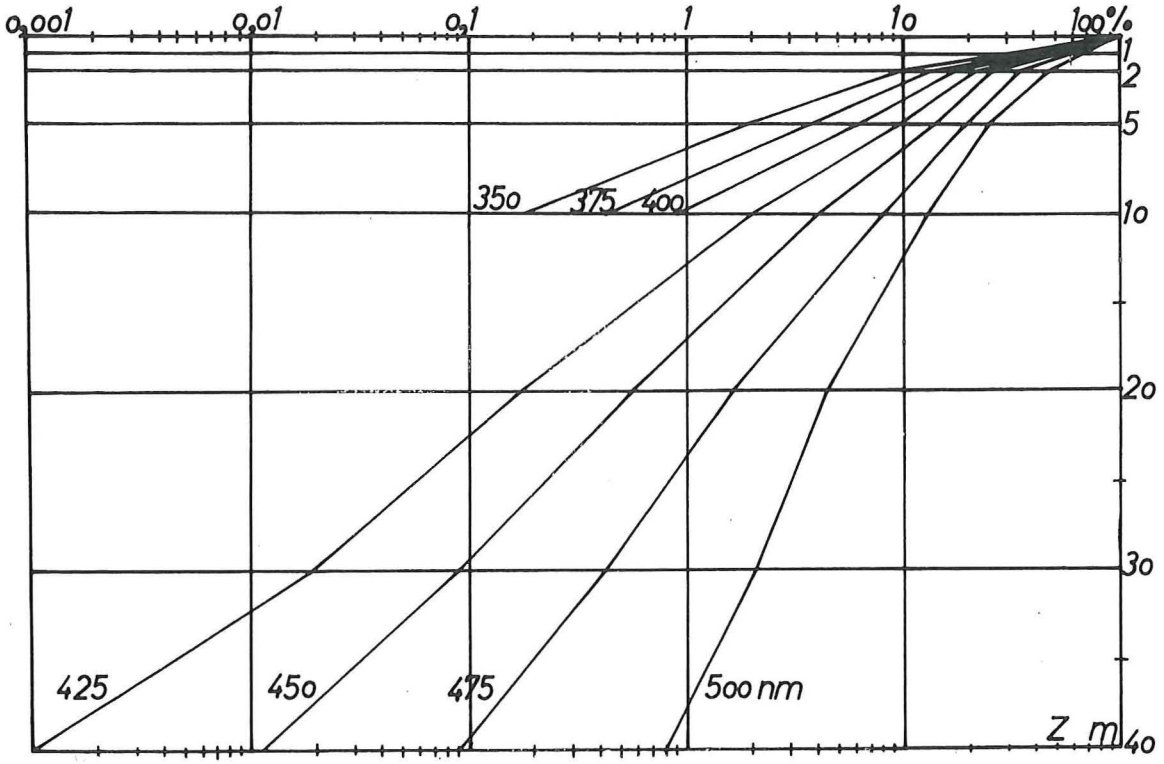

Fig. 18. St. 2. Vertical attenuation.

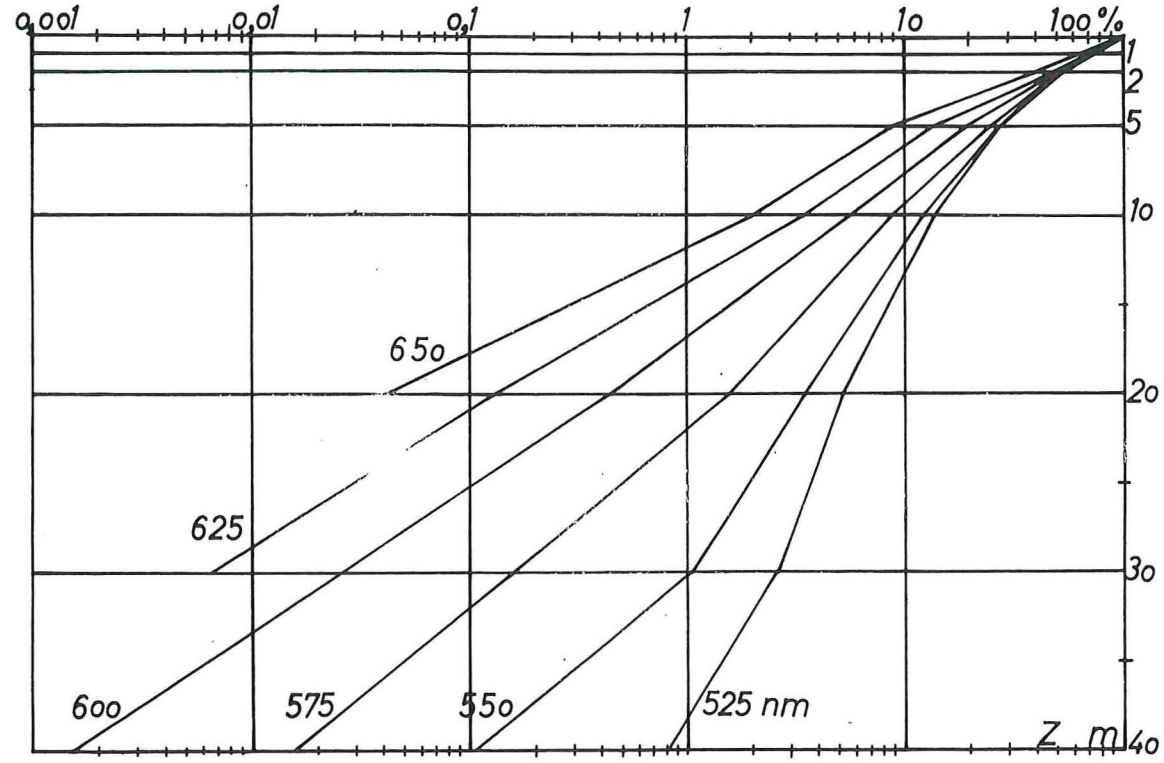

Fig. 19. St. 2. Vertical attenuation.

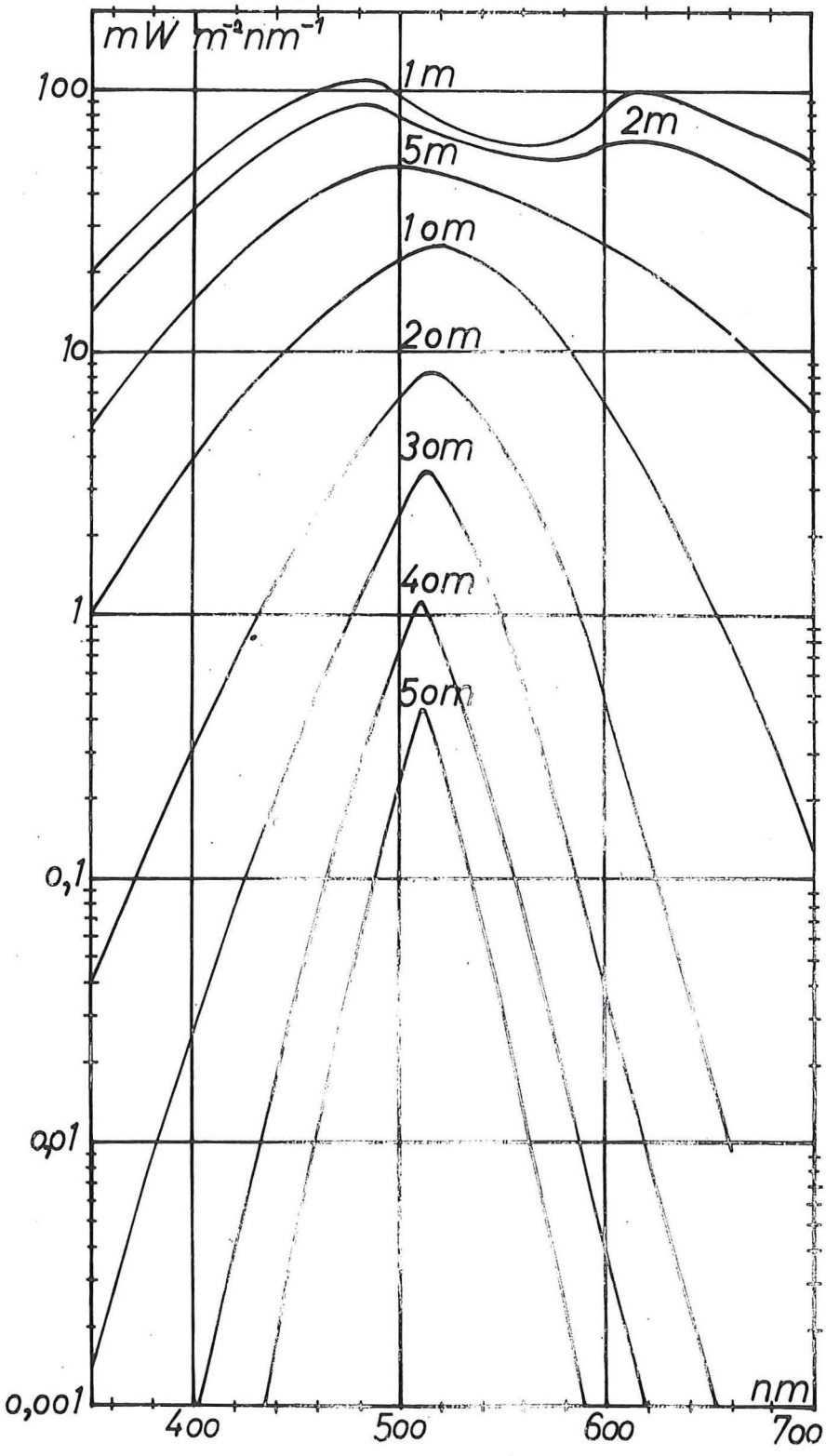

Fig. 20. St. 3. Irradiance.

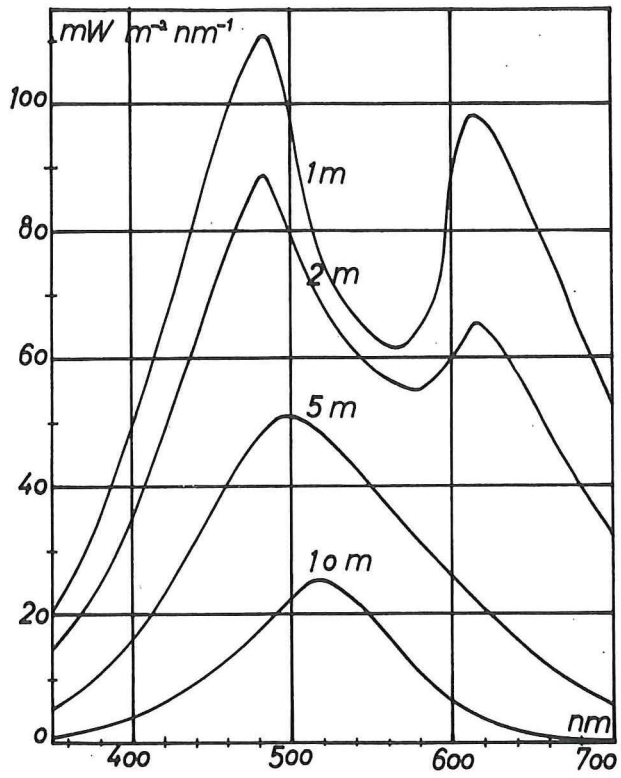

Fig. 21. St. 3. Irradiance.

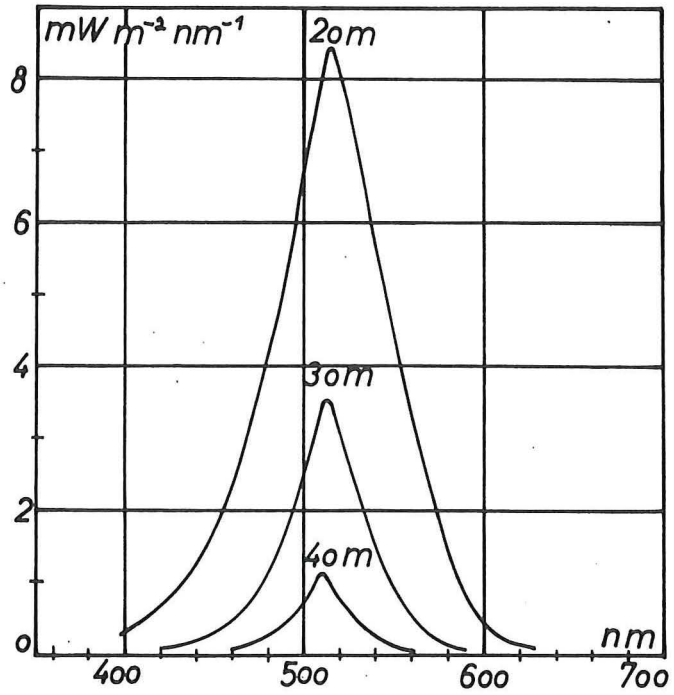

Fig. 22. St. 3. Irradiance.

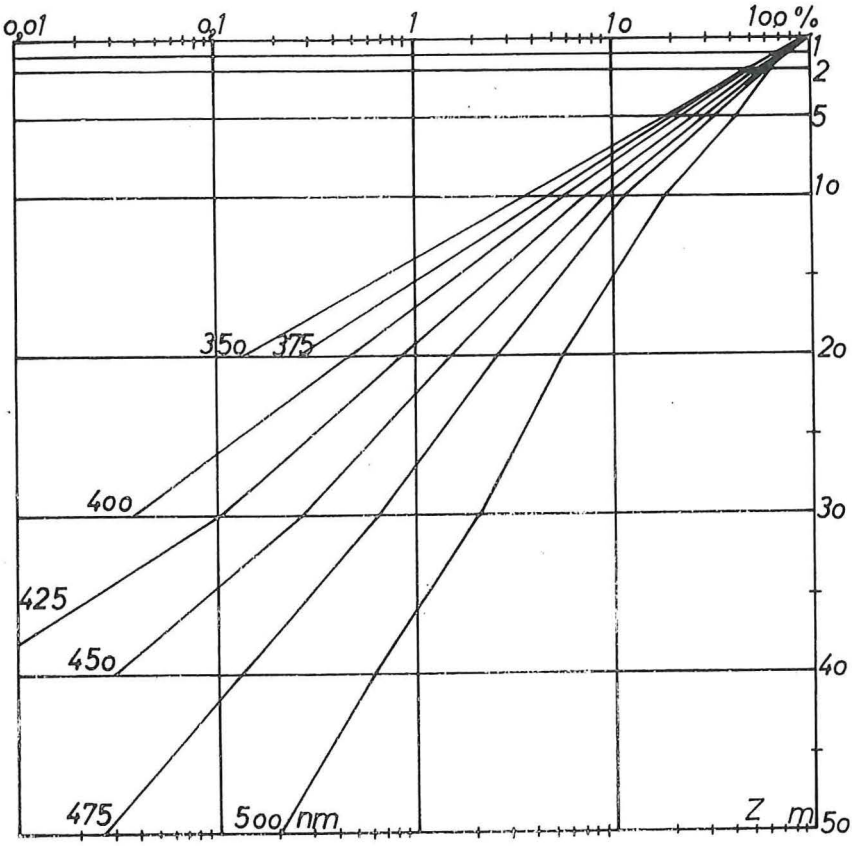

Fig. 23. St. 3. Vertical attenuation.

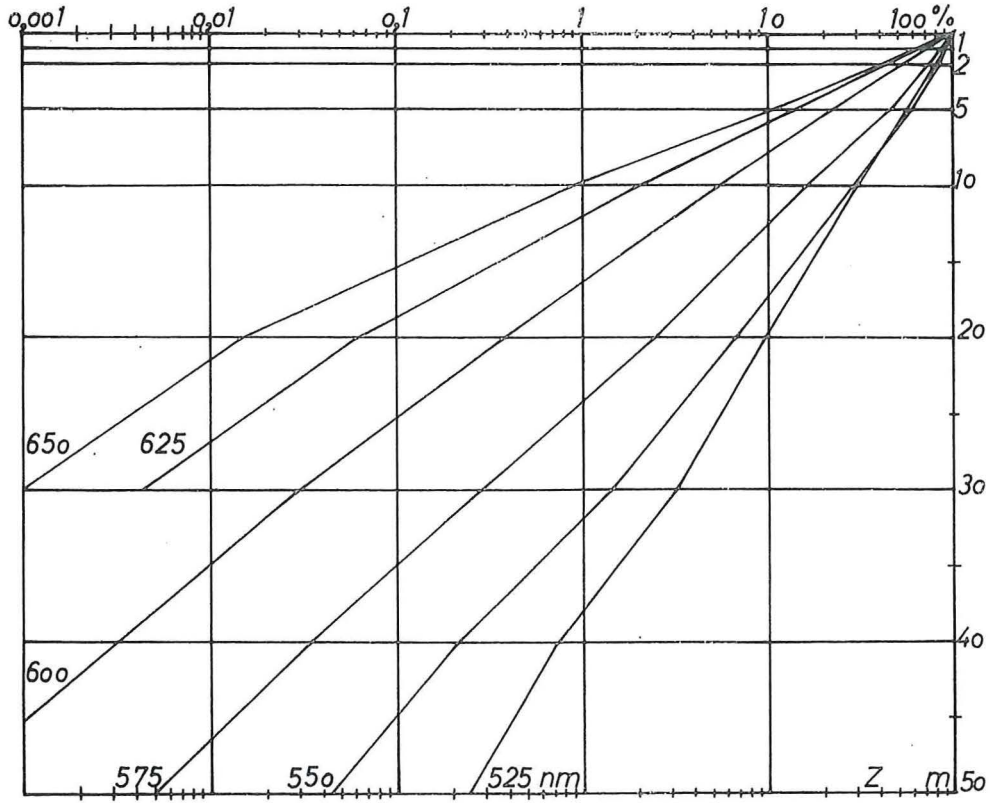

Fig. 24. St. 3. Vertical attenuation.

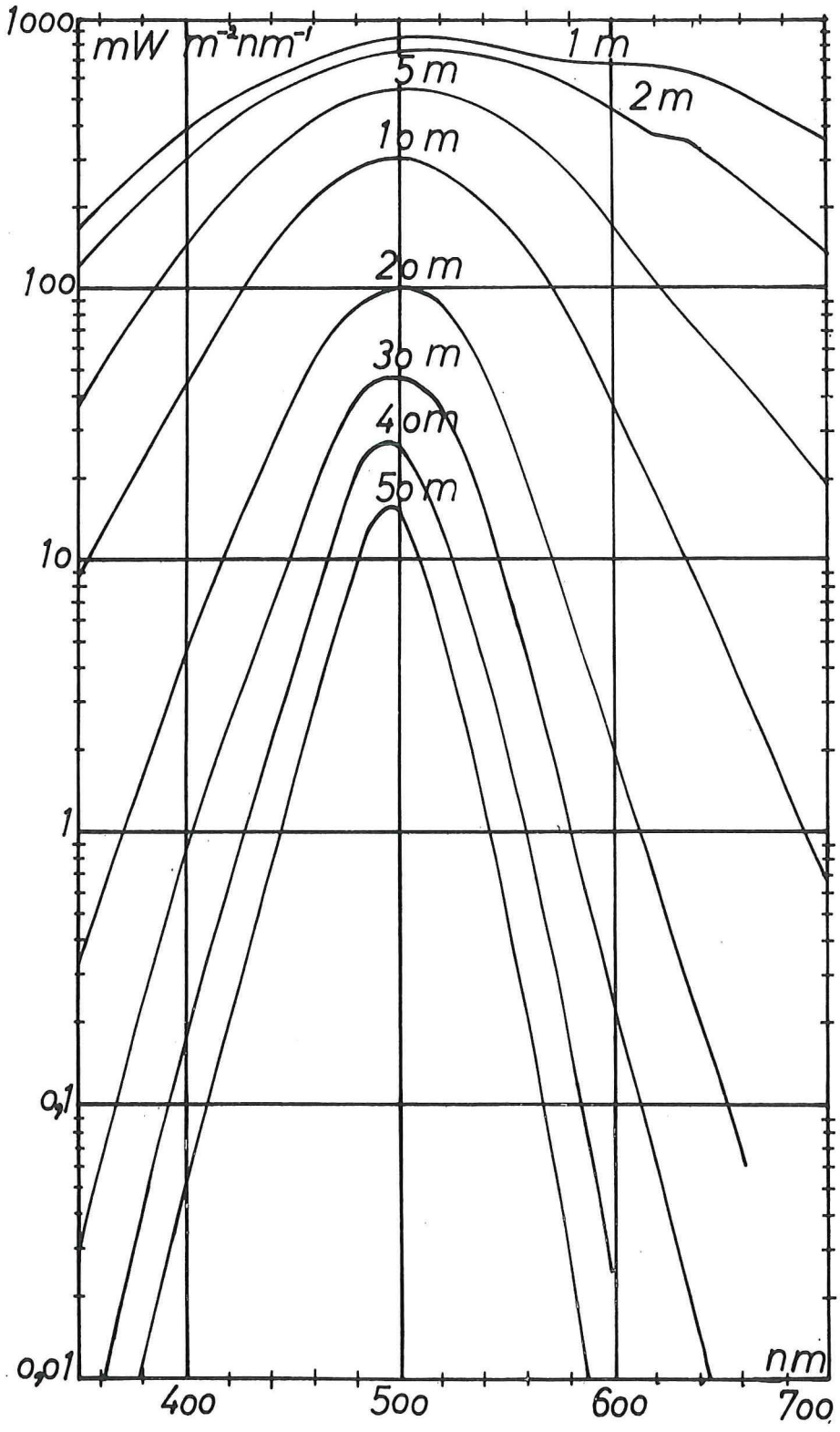

Fig. 25. St. 4. Irradiance.

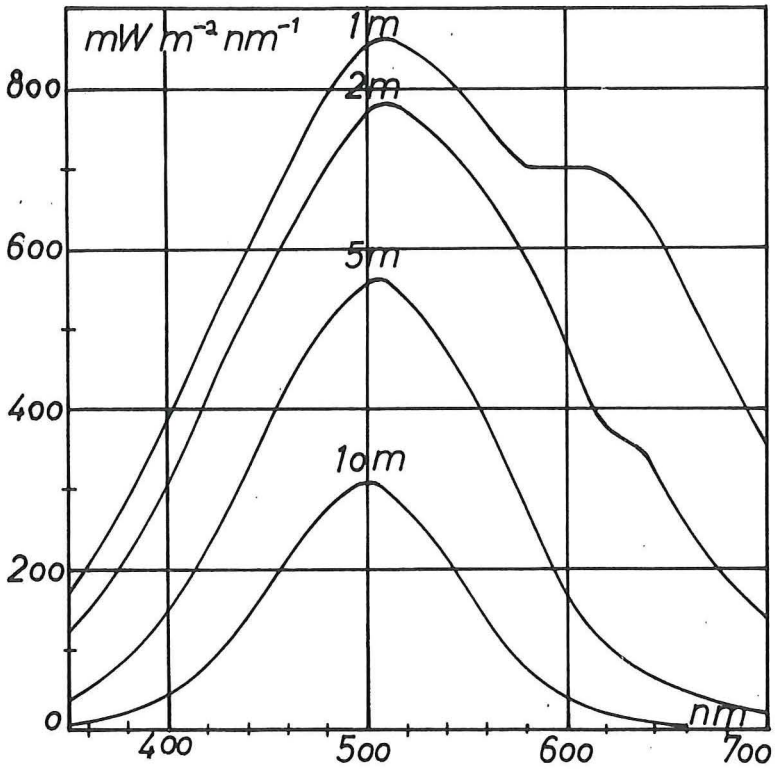

Fig. 26. St. 4. Irradiance.

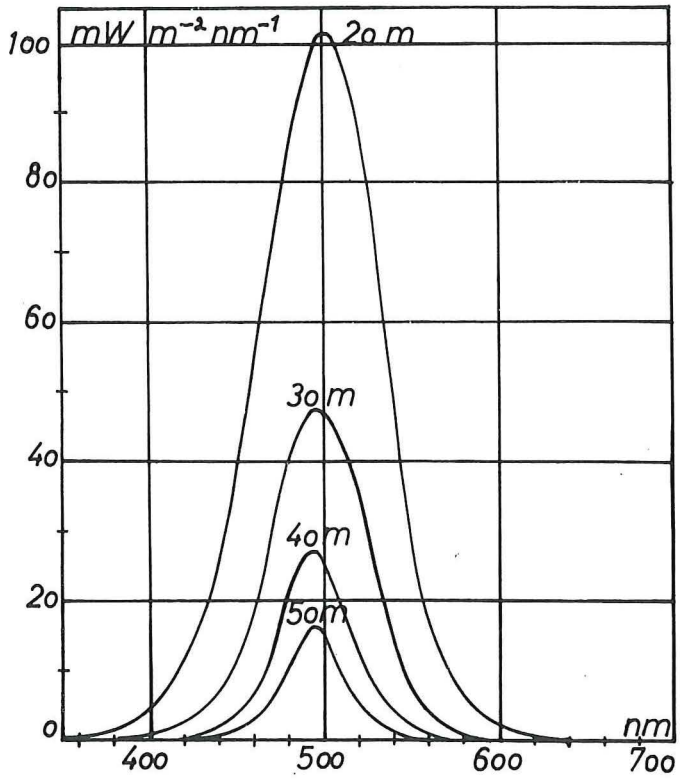

Fig. 27. St. 4. Irradiance.

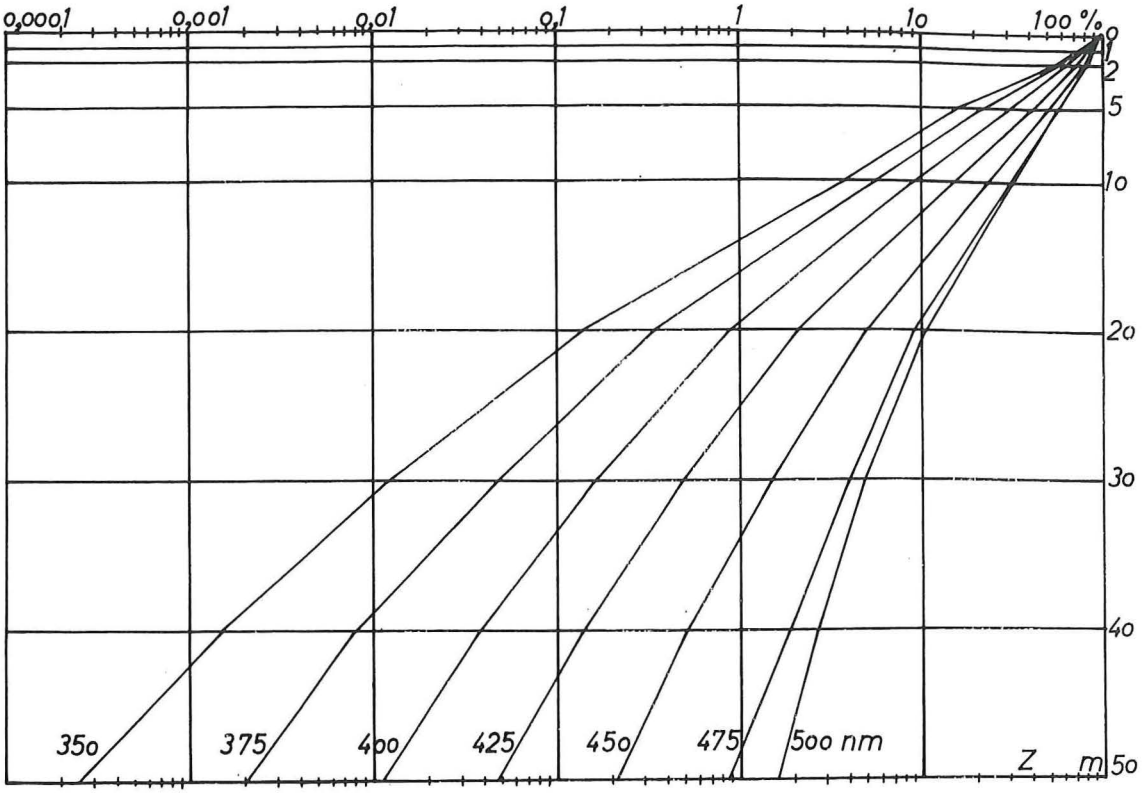

Fig. 28. St. 4. Vertical attenuation.

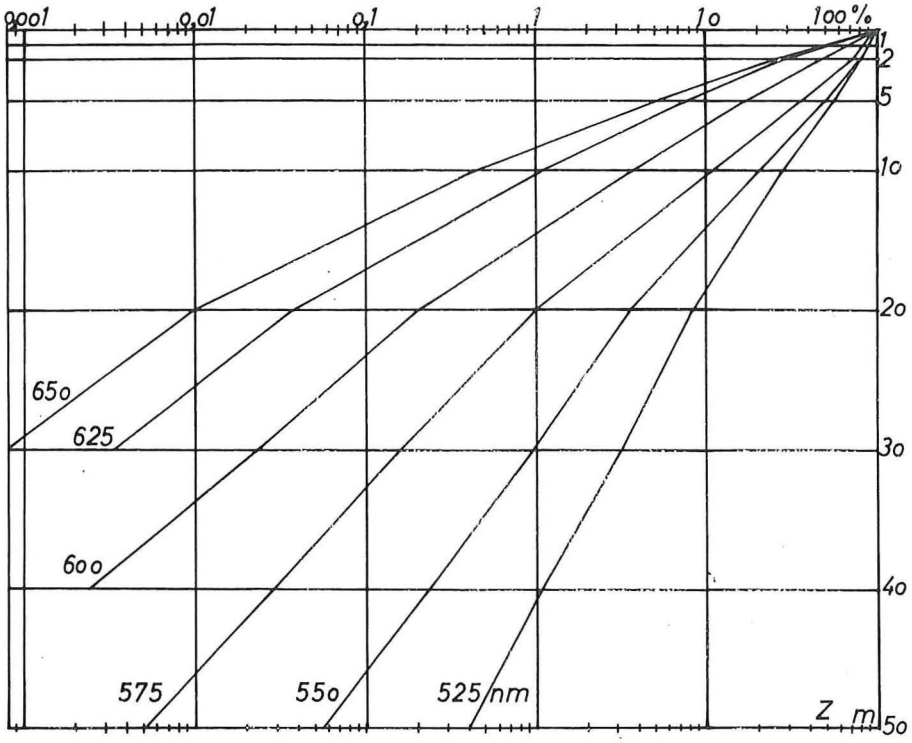

Fig. 29. St. 4. Vertical attenuation.

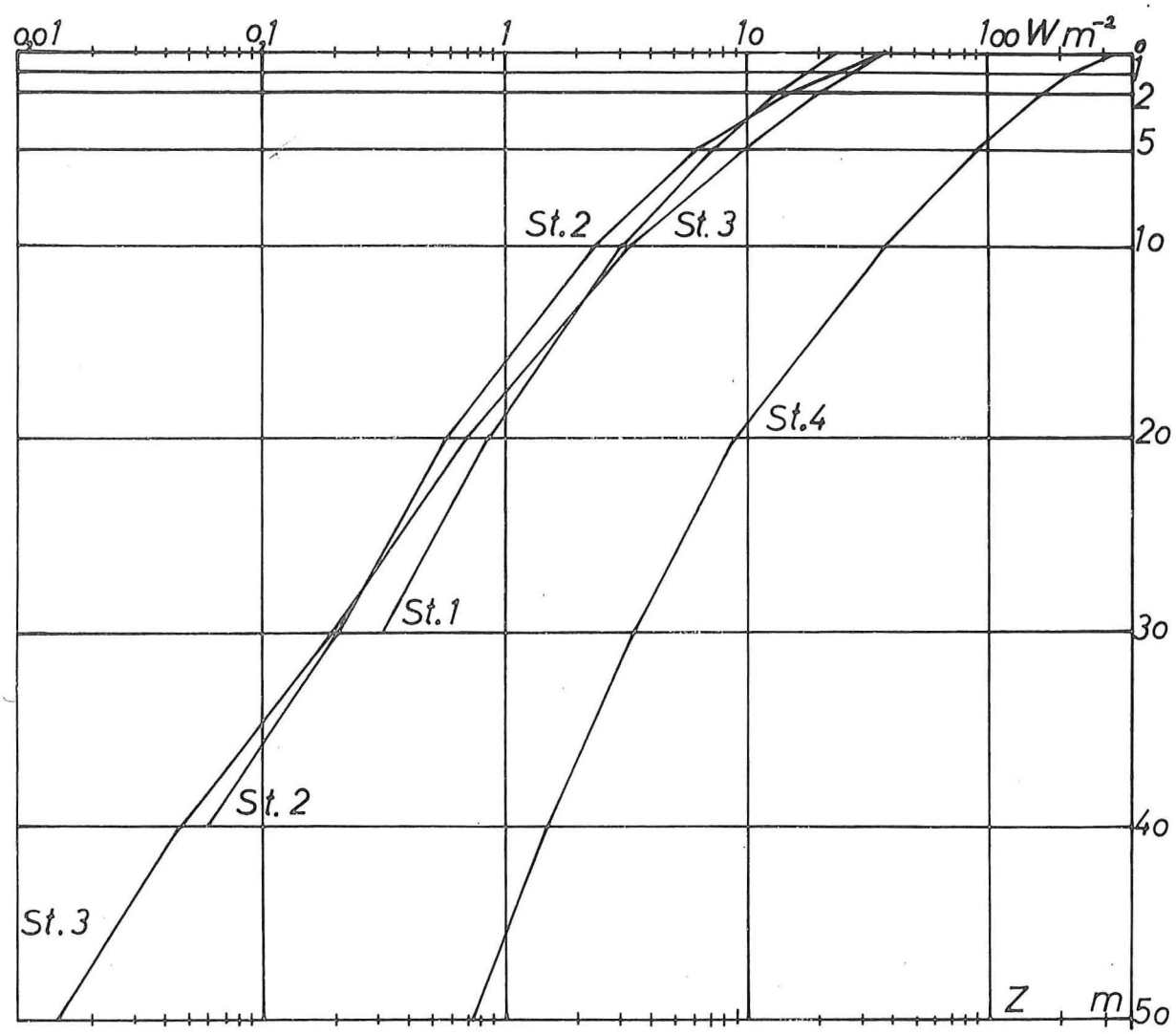

Fig. 30. Total irradiance (340-740 nm) of the stations.

This work is part of a Norwegian IBP project.
IBP has shared the expenses of the publication.